PROTEST

PROTEST FEE PAID
$15.00 24-05745
Fee Rec'd BY: ONLINE

November 15, 2024

RECEIVED
NOV 15 2024
WATER RIGHTS
ONLINE

Protestant: John Weisheit Living Rivers & Colorado Riverkeeper
PO Box 466
Moab, UT 84532

RE: Protest of Change Application a52233 (01-292)

A hearing is requested.

This water right application will cause harm to the public trust. The proposed infrastructure for municipal use will be compromised by high volume snow melts and maximum precipitation events in the Colorado River Basin.

Reference: A 2000 year natural record of magnitudes and frequencies for the largest Upper Colorado River floods near Moab, Utah. Noam Greenbaum et al., 2014. (attached to this complaint)

John Weisheit Living Rivers & Colorado Riverkeeper

Enclosure

SCANNED

AGU PUBLICATIONS

Water Resources Research

RESEARCH ARTICLE
10.1002/2013WR014835

A 2000 year natural record of magnitudes and frequencies for the largest Upper Colorado River floods near Moab, Utah

Noam Greenbaum[1], Tessa M. Harden[2], Victor R. Baker[3], John Weisheit[4], Michael L. Cline[5], Naomi Porat[6], Rafi Halevi[7], and John Dohrenwend[8]

[1]Department of Geography and Environmental Studies, University of Haifa, Haifa, Israel, [2]U.S. Bureau of Reclamation, Denver, Colorado, [3]Department of Hydrology and Water Resources, University of Arizona, Tucson, Arizona, [4]Living Rivers, Moab, Utah, [5]School of Earth Sciences and Environmental Sustainability, University of Northern Arizona, Flagstaff, Arizona, [6]Laboratory of Luminescence Dating, Geological Survey of Israel, Jerusalem, Israel, [7]Nehara, Misgav, Israel, [8]Deceased

Key Points:
- Forty four natural large floods occurred during the last two millennia
- Large floods are much more frequent than represented in the gaged record
- Conventional analysis underestimates the frequencies of extreme floods

Correspondence to:
N. Greenbaum,
noamgr@geo.haifa.ac.il

Citation:
Greenbaum, N., T. M. Harden, V. R. Baker, J. Weisheit, M. L. Cline, N. Porat, R. Halevi, and J. Dohrenwend (2014), A 2000 year natural record of magnitudes and frequencies for the largest Upper Colorado River floods near Moab, Utah, *Water Resour. Res.*, *50*, doi:10.1002/2013WR014835.

Received 11 OCT 2013
Accepted 8 JUN 2014
Accepted article online 11 JUN 2014

Abstract Using well-established procedures for paleoflood hydrology and employing optically stimulated luminescence (OSL) geochronology, we analyzed a very well-preserved natural record of 44 Upper Colorado River extreme floods with discharges ranging from 1800 to 9200 m^3s^{-1}. These are the largest floods occurring during the last 2140 $\pm$ 220 years, and this natural record indicates that large floods are much more frequent than can be estimated by extrapolation from the stream gaging record that extends back to 1914. Most of these large floods occurred during the last 500 years, and the two largest floods in the record both exceeded the probable maximum flood (PMF) estimated at 8500 m^3s^{-1} (300,000 cfs) for nearby Moab, Utah. Another four floods, with discharges greater than 7000 m^3s^{-1}, occurred during the last two millennia. Flood frequency analyses using the FLDFRQ3 model yields the following values, depending on the Manning ***n*** roughness coefficients: 100 yr flood—4670–4990 m^3s^{-1}; 500 yr flood—6675–7270 m^3s^{-1}; 1000 yr flood—7680–8440 m^3s^{-1}. The presumed PMF discharge (8500 m^3s^{-1}) gets assigned a recurrence interval of about 1000 years, and the largest historical 1884 flood (3540 m^3s^{-1})—a recurrence interval of $<$100 years. Flood frequency analysis for the Moab Valley based on the gaged record (1914–2012) yield 2730 m^3s^{-1} for the 100 yr flood and 3185 m^3s^{-1} for the 500 yr flood. This underestimation of the frequency of large floods from the gage data results from effects on that record by modern regulation of upstream river flow and associated water extraction for agriculture.

1. Introduction

The water resources of the Colorado River system are of immense importance for the economy of the southwestern U.S. In May of 1983, Colorado River flooding nearly threatened the failure of Glen Canyon Dam. Because such a failure would have immense consequences for the water security of the nation, it is important to have the best possible scientific understanding of the nature of flooding on that river system. We report here on the analysis of a remarkably complete and detailed natural record of the largest floods to have occurred on the Upper Colorado River in the last two millennia. That record was discovered near Moab, Utah, and we have analyzed it according to procedures established over the past 30 years in accordance with the science of paleoflood hydrology [*Baker*, 1987, 2008].

Data on the flood occurrences and magnitudes are conventionally derived from systematic measurements at gaging stations over time periods that are usually much less than 100 years. Additional data on high-magnitude historical floods along the Colorado River can be obtained from incomplete historical records that extend into the late 19th century. However, scientific advances over the past 30 years have made it possible to greatly extend the time scale for this database through paleoflood hydrology, which involves the combining of (1) geological synthesis of the sedimentary deposits and other paleostage indicators of ancient floods, and (2) hydraulic/hydrological analytical procedures [e.g., *Baker et al*., 1979; *Kochel and Baker*, 1982; *Baker*, 1987, 2008; *House et al*., 2002]. A paleoflood, as distinguished from a historical flood, is a past flood that has not been directly measured by modern hydrological procedures, as would be done at a stream gaging station, and it is also a flood that was not otherwise humanly observed and/or documented, as in the case of historical floods [*Baker*, 1987]. In essence, for paleoflood hydrology, it is the floods themselves that leave natural evidence of their occurrence, often in the form of sedimentary deposits, such as the slackwater deposits (SWDs) and other paleostage indicators (PSIs) that commonly occur in bedrock

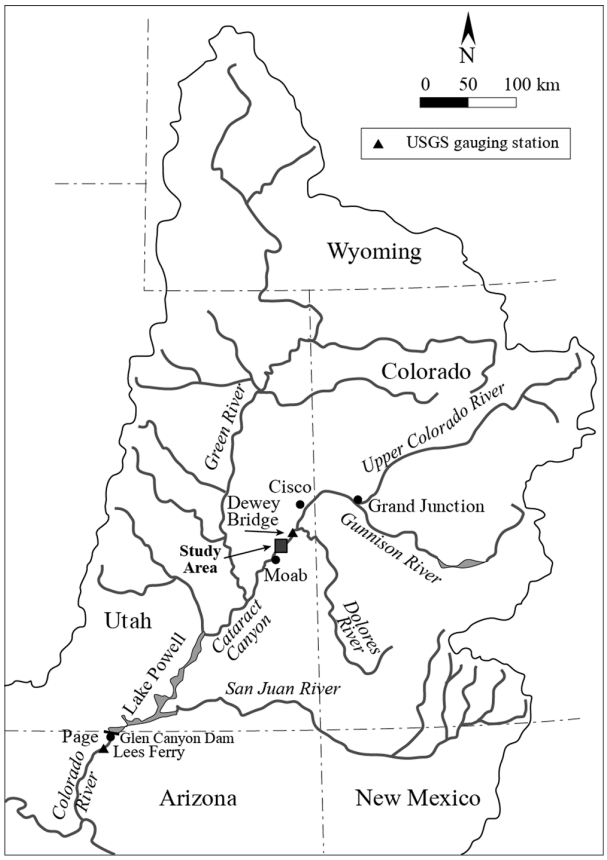

Figure 1. Upper Colorado River Basin including the larger tributaries, USGS gauging stations, and the present study area.

canyon environments [*Baker*, 1975; *Patton et al*., 1979]. The science of paleoflood hydrology exploits this natural recording of the most extreme floods by translating the SWD and PSI evidence into quantitative measures of the magnitudes and frequencies of the largest past floods over century and millennial time scales. By employing recent advances in quantitative geochronology, the ages of the SWDs and PSIs (and their causative flood events) can be obtained and incorporated into flood-frequency analyses.

Paleoflood hydrology has been extensively applied all over the world [*Baker*, 2006, 2013], and many studies have already been done for the larger Colorado River tributaries, including the Verde River [*Ely and Baker*, 1985], Salt River [*Partridge and Baker*, 1987; *Fuller*, 1987], Virgin River [*Enzel et al*., 1994], Escalante River [*Webb et al*., 1988], San Juan River [*Webb et al*., 2001], and the lower Colorado River at the Grand Canyon [*O'Connor et al*. 1994] (Figure 1). In a summary of all the measured, historical and paleoflood peak discharges for various tributaries of the Colorado River Basin *Enzel et al*. [1993] generated an envelope curve, which revealed that all the maximum measured (gaged) floods generally tend to be of lower magnitude than the historical floods and paleofloods.

The paleoflood study by *O'Connor et al*. [1994] was carried out downstream of Glen Canyon Dam and close to the USGS Lees Ferry gauging station (279,350 km^2; Figure 1). At that site, the largest measured flood of 6250 $m^3\ s^{-1}$, occurred in 1921, whereas the largest historical flood, with an estimated peak discharge of 8500 $m^3\ s^{-1}$, occurred in July 1884. A larger flood with an estimated peak discharge of about 11,300 $m^3\ s^{-1}$ probably occurred in 1862 [*Dickinson*, 1944]. The paleoflood record of *O'Connor et al*. [1994] provided evidence for at least 15 large floods during the last 4500 years. Ten floods during the last 2000–2300 years had discharges $> 6800\ m^3\ s^{-1}$; one flood, which occurred between about 1600 and 1200 years BP, was 24 m above present water level and had an estimated discharge of $> 14{,}000\ m^3\ s^{-1}$.

In the upper Colorado River close to the present study site in Moab, Utah (drainage area: 63,450 km^2), the conventional hydrological data are derived from the USGS gaging station at Dewey Bridge near Cisco (1914–2013; Figure 1). The present study was originally motivated by the scientific goal of testing risk estimates generated by conventional analysis of this gage record, e.g., *Kenny* [2004], for extreme flooding at a uranium mill tailings site on the right bank of the river as it enters the Moab Valley (Figure 2) [*Greenbaum et al*., 2006b; *Weisheit and Fields*, 2006]. In this study, we will supplement the conventional gage record of the Upper Colorado River with a newly discovered, long-term record of extreme paleofloods. We will then apply new flood frequency analyses (FFAs) to the combination of both the paleoflood hydrological data and the systematic data from the Dewey Bridge gage. The new paleoflood data and FFAs will be compared to the previous FFAs that were based on conventional hydrological methods alone. In essence, this study

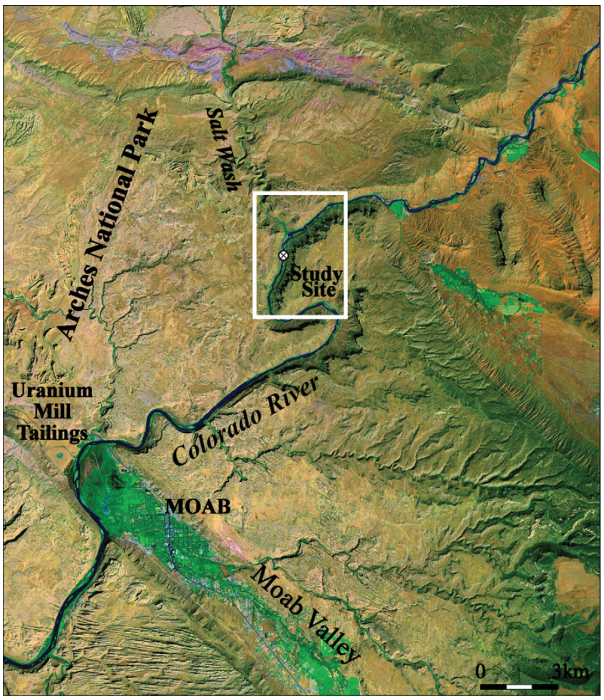

Figure 2. The location of the study area along the Colorado River Upper Colorado River in relation to Moab Valley and the Atlas uranium Mill Tailings [*Greenbaum et al.*, 2006b].

can be thought of as treating the engineering flood-frequency estimates as though they were scientific hypotheses as to the actual frequencies of rare extreme flooding on the Colorado River at this location, and then testing those hypotheses against the actual long-term record of extreme flooding presented by nature, i.e., the paleoflood record for that portion of the Colorado River.

1.1. Paleoflood Hydrology

Paleoflood hydrology provides long-term natural records of the magnitude and frequency for the largest past floods, thereby greatly extending the relatively short systematic flood records available from gaging stations [*Kochel and Baker*, 1982; *Baker*, 2003]. The documentation of the natural paleoflood records includes determination of (a) peak discharges based on paleostage indicators (PSI's) and slackwater deposits (SWDs); and (b) times of paleoflood occurrence, based on age dating, in this case by radiocarbon and optical stimulation luminescence (OSL). The paleoflood data enable (a) the documentation of the largest floods that occurred in a basin during a certain time period, (b) extension/establishment of hydrological records of hundreds and thousands years, and (c) enhancement of the frequency analyses of the flood records by an improved fitting of the probability functions [e.g., *Stedinger and Cohn*, 1986; *Webb et al.*, 1988; *Thorndycraft et al.*, 2003]. The flood frequency analysis (a) assumes that all floods above a certain threshold are recorded at the paleoflood site (b) combines and integrates various types of hydrological records including systematic, historical, and paleoflood. A review of various methods for incorporating paleoflood data and other nonsystematic information such as paleofloods into FFA and risk assessment is discussed by *Frances* [2004] and *Benito et al.* [2004].

Particularly reliable paleoflood data can be obtained from bedrock canyon environments, where cross sections, the course of the river, and channel gradient are all stable and can be assumed to be negligibly changed during the last hundreds and/or thousands of years. The paleoflood reconstruction uses fine-grained slackwater flood deposits (SWDs) deposited rapidly from suspension in sites where flow velocities are significantly reduced [*Baker et al.*, 1979; *Patton et al.*, 1979; *Kochel et al.*, 1982; *Ely and Baker*, 1985; *Baker*, 1987; *Baker and Kochel*, 1988], and other paleostage indicators (PSIs) such as driftwood lines. These indicators represent the minimum elevation of the high stage of the flood and provide an excellent natural record of flood magnitude. Such sites include back-flooded tributary mouths, caves, and alcoves in canyon walls, channel expansions where flow separation causes eddies, and overbank floodplain deposits. Ideal paleoflood sites preserve multiple flood stratigraphic records which can be separated into individual flow events using well-established sedimentological criteria [*Baker*, 1987; *Benito et al.*, 2003]. Paleodischarge estimates are obtained using the HEC-RAS [*Hydrologic Engineering Center*, 2005]—hydraulic procedure which generates water surface profiles for various discharge values [*O'Connor and Webb*, 1988]. Comparing the elevation of SWD's and driftwood lines to the elevations of the water surface profiles provides an estimate of the peak discharge for the flood deposit [*Baker*, 1987; *O'Connor and Webb*, 1988]. Ages of paleofloods are obtained using (a) radiocarbon dating of fine organic debris, wood, and charcoal which float over the

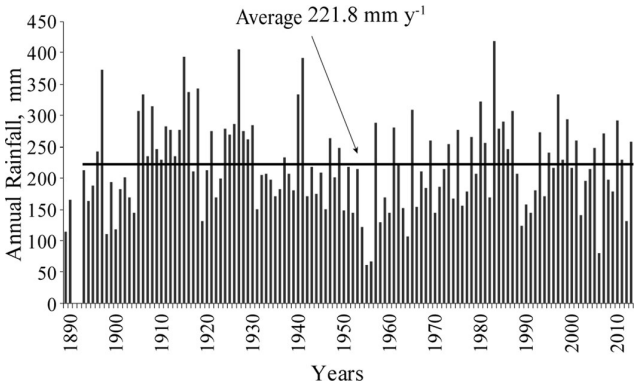

Figure 3. Annual rainfall in Moab, Utah—1889–2013. Mean annual rainfall for the period 1893–2013—221.8 mm yr^{-1}. The mean annual rainfall for the periods 1893–1960 and 1960–2013 are almost the same—222.9 and 220.6 mm yr^{-1}, respectively.

floodwaters and deposited over the flood SWD or as a driftwood line (b) Optical Stimulation Luminescence (OSL) for the fine sandy fraction of these suspended sediments.

2. Study Area

2.1. Climate and Hydroclimate of Floods

The region is arid to semiarid with maximum monthly average temperatures occurring in July, varying between 17.8 and 37.2°C, and minimum monthly average temperatures occurring in January, varying between −6.7°C and 6.1°C. Annual rainfall in Moab gaging station (1889–2013) at an elevation of about 1280 m, ranges between 110 and 417 mm y^{-1}; mean annual rainfall for the period 1889–2013 is 221.8 mm y^{-1} (Figure 3). Precipitation is evenly distributed throughout the year, with some of it falling as snow during the winter. The maximum monthly average rainfall of 29 mm occurs in October, whereas the minimum monthly average of 10 mm occurs in June. Some of the wettest years on record—1905, 1941, 1965, and 1983—are related to El Nino Southern Oscillation (ENSO) activity [*Webb and Betancourt*, 1992*; Ely et al*., 1993*; Cayan and Webb*, 1993; *Anderson*, 1993]. Other wet years are related to positive values of the Pacific Decadal Oscillation (PDO) index [*Webb et al*., 2004].

Spring floods in the upper Colorado River are mainly caused by melting of the snow pack during the first waves of relatively high temperatures, which results in annual peak discharges that usually occur between May and June and are characterized by moderate rates of hydrograph rise and recession. Large flood-producing rainstorms in the Colorado River basin are related to two major climatic conditions, mainly during winter [*Ely et al*., 1994]: (a) Winter North Pacific frontal storms and (b) Late summer and fall storms associated with Pacific tropical cyclones over northern Mexico in conjunction with a midlatitude low-pressure trough. These two storm types are associated with multiple-year periods dominated by negative Southern Oscillation index (SOI) or El Nino conditions [*Webb and Betancourt*, 1992; *Cayan and Webb*, 1993]. Finally, there are localized summer thunderstorms, which typically occur in July–August and generate small floods with steep rising limbs and short recessions. Especially large floods may occur when spring rainstorms coincide with the melting snowpack. Rainfall intensities during flood-producing rainstorms in Utah during the 1920s–1930s exceeded values of 22.9 mm per 10 min (7 July 1933) and about 24.4 mm per 35 min (11–13 August 1923) [*Woolley*, 1946].

2.2. Stream Flow Data

Conventional stream flow data for present study area come from the USGS gauging station in Dewey Bridge near Cisco (30 km upstream of the study area; Figure 1). The drainage area of the Colorado River at the station is 62,470 km^2. The flood record at this station begins in 1914 and is continuous except for the period 1918–1922 (Figure 4). Maximum annual peak discharges range from 185 $m^3 s^{-1}$ in 2002 to 2175 $m^3 s^{-1}$ in 1917 with an average of 987 $m^3 s^{-1}$. The maximal measured peak discharge of 3540 $m^3 s^{-1}$ is for a historical flood that occurred in April 1884.

Historical floods in the Colorado River, prior to 1884, were estimated only downstream of Moab in Cataract canyon (Figure 1) because the Moab Valley was not then populated. In Cataract canyon downstream of the confluence between the Colorado River and the Green River, a large flood with an estimated peak discharge of about 6370 $m^3 s^{-1}$ occurred in June 1884, but it is unclear how large this flood was at the Upper Colorado River near Moab. The existing flood records in the Upper Colorado River indicate that numerous large floods occurred between the 1880's and the 1930's, but since then, there has been a general decreasing trend (Figure 4). A comparison of the average peak discharge for the period 1914–1960—1202 $m^3 s^{-1}$ with

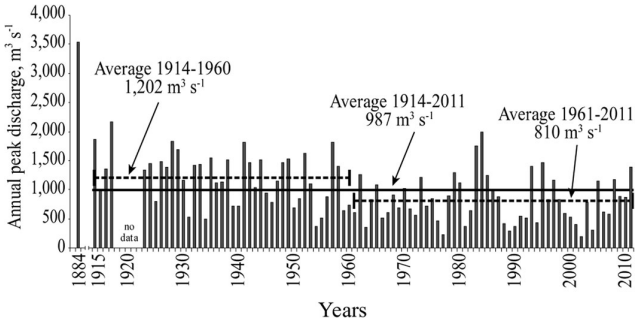

Figure 4. Annual maximum peak discharges in the Colorado River at the Dewey Bridge gauging station near Cisco, Utah 1914–2011 (average max. peak discharge—987 m^3s^{-1}). Comparison between the average peak discharge for the period 1914–1960 (1202 m^3s^{-1}) versus 1960–2011 (810 m^3s^{-1}) indicates a clear decrease by about 30%.

the period 1960–2011—810 m^3s^{-1} shows a clear reduction by about 33%. During the period 1914–1960, 11 floods of >1500 m^3 s^{-1} occurred versus only two such floods during the period 1960–2012 (Figure 4). *Webb et al*. [2004] explained this trend by (a) land-use changes mainly—the abrupt reduction in grazing since 1932, (b) the regulation of the river for agriculture and the resulting increase in water extraction [*U.S. Bureau of Reclamation*, 2003] (Figure 5), and (c) a possible decrease in the frequency of large flood-producing rainstorms since the early 1940s. *Kenney* [2004] analyzed the hydrological record at Dewey Bridge and estimated the 100 year flood at 2765 m^3s^{-1}, and the 500 year flood at 3400 m^3s^{-1}. The Probable Maximum Flood (PMF) for the Moab Valley was calculated at 8500 m^3s^{-1} (300,000 cfs). Mean annual flow volume is about 6660 $\times$ 10^6 m^3.

2.3. Study Site

The Colorado River at the study area is deeply entrenched into the Glen Canyon Group and into the underlying Triassic Chinle Formation, resulting in an impressive bedrock canyon. The northwestern bank is undisturbed and is a part of the Arches National Park (Figure 2), whereas the historical road along the river corridor is located at the southeastern bank. The study area is located about 17 km upstream of Moab at a large bend of the canyon (Figure 2), where the drainage area is 63,450 km^2. The elevation of the River bed at the study area is about 1300 m a.s.l. The channel width varies between 70 and 150 m, depending on the geometry of the cross section and discharge. The constrictions in the channel are usually caused by very coarse debris flows derived from the steep slopes of the canyon, which also forms small rapids [*Webb et al*., 1988, 2004]. The general gradient along this section is about 0.0017.

The study site was selected based on satellite images and air photos, overflights, and field reconnaissance. Three potential paleoflood sites were located along a study reach of about 5 km long, between Sandy Beach and Big Bend (Figure 6). The best of the three sites selected for the study, BLM-TO, is located a few hundred meters upstream of the boat take out point at the right bank of the River. This overbank SWD site overlies an alluvial terrace composed of coarse gravel—cobbles and boulders. The site was chosen because of good SWD preservation on the undisturbed right bank of the river and indications of long-term stabilization of the sediments. The site also affords minimal issues for digging and trenching. The other two sites—COL-1 and COL-3 (Figure 6)—are covered by a thick layer of aeolian sand and therefore are suspected to be partially reworked flood deposits.

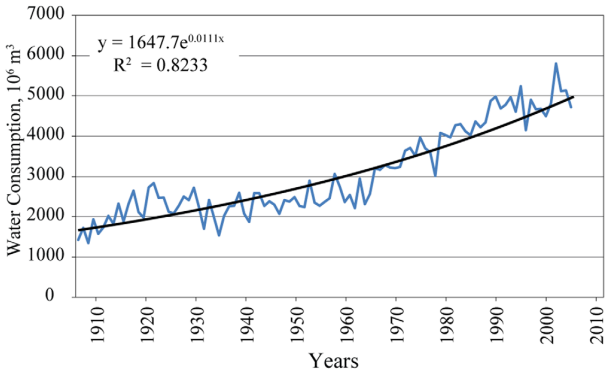

Figure 5. Annual water consumption at the Colorado River basin (including evaporation), upstream of Lees Ferry, Arizona (279,350 km^2) for the period 1906–2004. Water consumption increased from about 1400 10^6 m^3 yr^{-1} in 1906 to >5000 10^6 m^3 yr^{-1} in the earlier 2000s (3–4 times). (Source: James Prairie, Bureau of Reclamation, U.S. Department of the Interior, http://www.usbr.gov./lc/region/g4000/NaturalFlow/index).

3. Methods

3.1. Field Methods

3.1.1. Field Survey

We conducted a survey along the 4.5 km study river reach from

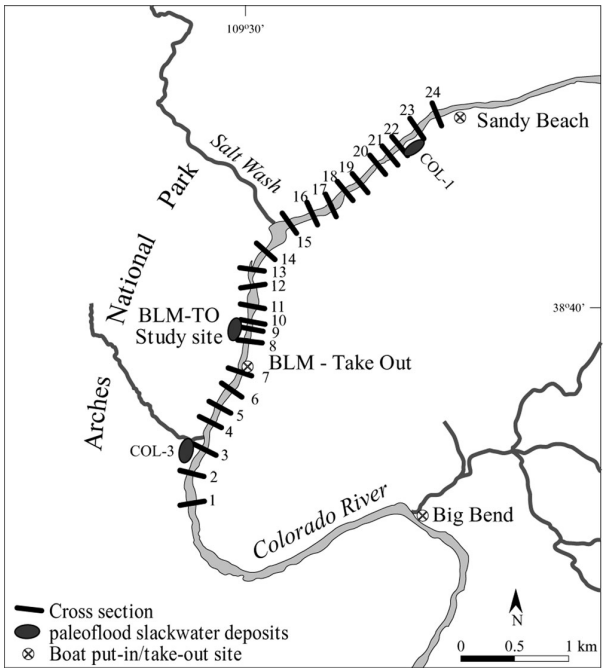

Figure 6. The study reach including the main slackwater deposits (SWD) accumulations, location of the cross sections, and the paleoflood BLM-TO study site.

Sandy Beach and downstream almost to Big Bend (Figure 6) using an EDM total station with a laser rangefinder to generate 24 cross-sections, spaced approximately every 180–190 m. The measurements included all relevant geometric parameters of the channel and the adjacent canyon of the Colorado River including width, elevations above water level during the period of the survey (May 2005), gradient, sinuosity, elevations, and locations of all paleostage indicators (PSIs), such as driftwood lines and slackwater deposits (SWDs). These indicators serve as evidence for the actual or minimal water stages of past floods. Roughness coefficient—Manning ***n*** was estimated for the water surface and for the banks of each cross section above water level.

3.1.2. Sedimentological Methods

Fourteen pits up to 2 m deep were dug in the flood deposits down to the underlying boulders of the alluvial terrace (Figure 7). The pits were dug close to each other with a vertical overlapping that enabled a staircase exposure of the entire section of the SWD sequence from top to bottom as well as correlation between sedimentary units in adjacent pits. The deposits exposed in each pit were separated into sedimentary units associated with flood events using the well-established sedimentological criteria [*Baker*, 1987; *Kochel and Baker*, 1988; *Benito et al*., 2003], thereby enabling a documentation

Figure 7. Paleoflood slackwater deposits at the study site. The numbers represent the stratigraphy pits. Pit no. 1 (with a nearby person for scale) is the highest flood deposit—about 15 m above the water surface (425 $m^3 s^{-1}$, June 2005). Note the high water marks of the observed 25–26 May 2005 flood—peak discharge of 1140 $m^3 s^{-1}$ [*Greenbaum et al*., 2006b].

Table 1. Results of Radiocarbon Dating of Paleflood Deposits at the BLM-TO Site (95.4% Probability), Using OxCal 4.2 [*Bronk Ramsey*, 2009, 2013][a]

Sample No.	Pit No.	Flood Deposit No.	Material	^{14}C Age (Years)	Calibrated Age (Years AD/BC)
A13878	4	3	Wood	135 ± 35	1669–1945 AD
AA65420	10	5	Charcoal	340 ± 34	1467–1641 AD
A13879	13	2	Wood	120.5 ± 1.8	1950–present
A13877	14	5	Soil	6275 ± 160	5532–4842 BC

[a]Sample A13877 dated Total Organic Carbon of a soil and came out extremely old although it overlies units that are a few hundred years old only. Therefore, we assume that the sample contained older carbon and the age does not represent the actual chronology. The sample was therefore ignored.

of the stratigraphy at each pit. Each depositional unit at each pit was documented in detail and at each pit, between 1 and 3 units, were sampled for potential age dating. The sampled material for radiocarbon dating consisted of wood or charcoal that had floated in the floodwaters to be deposited with a flood SWD unit, usually as a discontinuous thin layer at the unit top or as small chunks within the unit. However, because of the very limited amounts of organic matter, most of the systematic sampling was for optical stimulated luminescence (OSL) dating.

3.1.3. Underwater Survey

Complementary underwater cross sections, using a sonar type LOWRANCE X59DF, were surveyed in 2010 for 17 out of the 24 cross sections along the study reach. The water surface during this set of measurements was lower (discharge of 260 $m^3\ s^{-1}$) than during the previous set of measurements in 2005 (discharge 1140 $m^3\ s^{-1}$). Seven EDM—surveyed data points were added to each cross section—2 points at the contact of the water surface and the banks and another 5 underwater points, spaced about every 7–17 m. This survey documents the depth of the water down to the channel bed thereby completing the underwater geometry of the cross sections.

3.2. Dating Methods

3.2.1. Radiocarbon

Most of the organic material for radiocarbon dating was extracted from thin, discontinuous organic layers at the top of the deposits or from charcoal chunks within the flood deposit. Our dating techniques employed conventional scintillation counting, accelerator mass spectrometry (AMS), and postbomb dating for the modern floods, i.e., younger than 1950 AD [*Baker et al*., 1985; *Ely et al*., 1992]. The samples were analyzed at the Radiocarbon and Isotope Laboratory, Department of Geosciences, University of Arizona and at the AMS Laboratory, Department of Physics, University of Arizona (Table 1).

3.2.2. Optical Stimulated Luminescence (OSL)

The fine, sandy sediments of the Colorado River are ideal for luminescence methods [*Aitken*, 1998] that date the last exposure episode to sunlight in a mineral grain's history and measure signals that are acquired by the grains from the natural environmental radiation. The magnitude of the OSL signal is related to the total radiation that the sample received. Since the OSL signal is sensitive to sunlight, exposure to the sun during transport and deposition of the sediment will reduce the previously acquired OSL signal to zero ("bleaching"), and after burial it will grow again. Fine sand-size quartz is ideal for this technique, and it was extracted using routine laboratory procedures [*Porat*, 2002]. The equivalent dose (De) was measured using the OSL signal, and the single aliquot regenerative dose (SAR) protocol [*Murray and Wintle*, 2000] was followed on 12–18 aliquots for each sample. Our systematic sampling of the sandy SWD units yielded, wherever possible, 1–3 OSL samples per a pit, usually at the base of the pit and >0.5 m below the surface. This resulted in 12 samples (Table 2) that were analyzed at the Luminescence Laboratory of the Geological Survey of Israel (GSI) in Jerusalem.

3.3. Hydraulic Methods

Three types of hydraulic analyses were applied to the geometric and hydraulic data derived from 24 cross-sections along the 4.5 km study reach:

(a) Preliminary estimates of the paleodischarges of the floods were calculated in three cross sections (XSs 8,9,10 in Figure 6) using the slope-area method, while channel bed topography and depth were unknown [*Greenbaum et al*., 2006b]. This discharge calculation presumed the water surface during the survey to be a

Table 2. Results of OSL Dating of Paleoflood Deposits at the BLM-TO Site, Colorado River[a]

Sample	Depth (m)	K (%)	U (ppm)	Th (ppm)	Ext. α (μGy/a)	Ext. β (μGy/a)	Ext. γ (μGy/a)	Cosmic (μGy/a)	Total Dose (μGy/a)	De (Gy)	Age (Years)
P2U5	40–50	1.66	2.05	6.7	8	1492	903	214	2617 ±4 7	3.68 ± 0.27	1410±110
P4U4	110–120	1.99	2.90	9.2	11	1870	1182	182	3245± 56	6.95 ± 0.71	2140±220
P5U1	40–50	1.74	2.50	8.4	10	1639	1046	214	2909 ± 51	3.79 ± 0.26	1300±90
P5U2	70–80	1.74	2.50	8.6	10	1643	1055	193	2901 ± 51	4.24 ± 0.22	1460±80
P9U5	90–100	1.58	1.97	5.8	7	1388	816	186	2397 ± 64	0.92 ± 0.24	390±100
P10U3	50–60	1.58	2.30	7.4	9	1487	942	207	2645 ± 46	0.45 ± 0.12	170±40
P10U7	100–110	1.66	1.80	5.5	7	1434	822	184	2447 ± 45	1.01 ± 0.18	410±70
P11U5	90–100	1.58	2.15	7.2	9	1464	917	186	2576 ± 46	0.58 ± 0.15	230±60
P12U5	90–100	1.74	2.58	8.3	10	1646	1050	186	2892 ± 51	1.40 ± 0.45	490±150
P13U6	70–80	1.49	2.53	7.5	10	1458	951	193	2611 ± 47	0.57 ± 0.19	220±70
P14U7	60–70	1.66	4.20	7.7	13	1779	1177	199	3168 ± 55	1.46 ± 0.34	460±110
P14U13	170–180	1.83	4.50	10.8	16	1998	1388	169	3570 ± 61	0.73 ± 0.22	200±60

[a]Gamma dose rate was calculated from the radioelements and the cosmic dose estimated from burial depth. Water content was estimated at 5%. Quartz with grain size 125–150 μm was etched by concentrated HF for 40 min following dissolution of carbonates by HCl. De was obtained on 12–18 aliquots per sample using the single aliquot regeneration (SAR), with preheats of 10 s at 200–260°C. Test dose was ~4.5 Gy and a cut heat of 5s @180°C was used. Ages are in years before 2010.

smooth channel bed. Manning's ***n*** was estimated as 0.025 for the channel due to the low roughness of the water surface; and as 0.06 for the adjacent banks and hill-slopes due to their rugged nature and coarse texture (cobbles and boulders) and the dense vegetation of the narrow floodplain and nearby foot slope [*Webb et al*., 2004].

(b) A HEC-RAS hydraulic computer model [*Hydrologic Engineering Center*, 2005] was used to generate water surface profiles (WSP), using step-backwater calculations for various discharge values [*O'Connor and Webb*, 1988; *Webb and Jarrett*, 2002]. Comparing the elevations of the SWDs and PSIs to the computed elevations provides a minimal estimation of the peak flood discharge that emplaced those indicators.

(c) Finally, a HEC-RAS analysis was done for the entire cross sectional geometry, incorporating the underwater data surveyed in 2010. The elevations of the observed water surfaces (OWS) during the surveys were documented and discharges associated with each were used for model calibration. The calibration flows were measured at the Dewey Bridge gauging station, as follows: 1140 $m^3 s^{-1}$ on 25–26 May, 2005; 425 $m^3 s^{-1}$ on 13–14 June, 2005; and 260 $m^3 s^{-1}$ on the 26–27 June, 2010.

Comparisons of SWD elevations with other field observations, such as the elevation of driftwood lines of the same floods, historical water levels, and gauged discharges, indicate that the elevation of the slack water deposits is usually lower than the actual peak stage [*Kochel et al*., 1982; *Ely and Baker*, 1985; *Baker*, 1987; *Partridge and Baker*, 1987; *O'Connor et al*., 1986]. This difference exceeds 50–70 cm for the largest measured floods in Nahal Zin, a 1400 km^2 ephemeral stream in the Negev Desert, Israel [*Greenbaum et al*., 2000]. This would lead to an underestimation of the peak discharge and they should therefore be treated as minimum values [*Kochel et al*., 1982; *Baker*, 1987].

Water surface profiles for large floods in relatively narrow bedrock-controlled streams typically indicate that flows are generally in the subcritical regime [e.g., *Ely and Baker*, 1985; *Partridge and Baker*, 1987; *O'Connor et al*., 1986; *Baker*, 1987; *O'Connor and Webb*, 1988; *Wohl*, 1998; *Greenbaum et al*., 2006a]. Supercritical conditions are reached only rarely and in few locations, generally where the channel gradient increases abruptly, such as large cataracts and rapids, or downstream of abrupt constrictions, again depending on the discharge.

Other uncertainties for paleoflood hydrology discharge calculations are discussed in detail by *O'Connor et al*. [1994] and include: (a) flow conditions downstream of the study reach and their effect on the local surface profiles; (b) values for the energy loss coefficients, and (c) channel geometry during peak flow stages. Inaccuracy in the discharge estimations may also result from the selected hydraulic roughness coefficient; studies of Manning's ***n*** choice for calculating very large discharges in narrow, deep bedrock canyons show low sensitivity [*O'Connor and Webb*, 1988; *Wohl*, 1998]. Our present study, employed a variety of Manning ***n*** coefficients ranging from 0.015 to 0.04 for the channel and 0.045 for the bank to produce various hydraulic scenarios in order to choose those that best fit to the measured data, mainly the 1140 $m^3 s^{-1}$ of May 2005 flood (Figures 8 and 9). The two better sets were used for the iterations of WSP's for discharges of 1140–3500 $m^3 s^{-1}$. The two sets were: (a) Manning ***n*** of 0.028 for the channel and 0.045 for the banks (scenario 2)

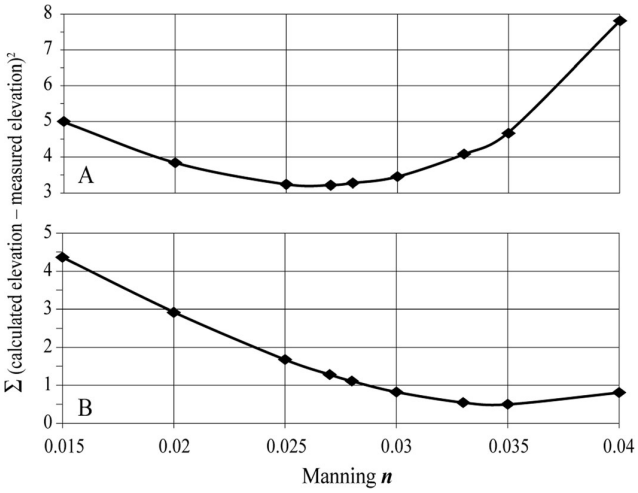

Figure 8. The best fit between the measure and calculated elevation of the water surface for a discharge of 1140 m^3s^{-1} (observed, May 2005 flood; see also Figure 9) using the sum of the square differences between them. The best fit was tested for the following scenarios of Manning ***n*** roughness coefficients: channel—0.015, 0.02, 0.025, 0.027, 0.028, 0.03, 0.033, 0.035, and 0.04; banks—0.045 for all except for the channel Manning ***n*** of 0.035 for which we used 0.035 for the banks [*Magirl et al*., 2008]. The test was applied to the lower segment of the study reach below the lowest control section (Figure 9) in which the study site is located, on the following subsegments: (a) cross sections (XS's) 1–14 and (b) XS's 1–10. The best fit to subsegment (a) is Manning ***n*** roughness coefficients of 0.027–0.028 for the channel and 0.045 for the banks, whereas for subsegment (b) the best fit is Manning ***n*** roughness coefficient of 0.035 for both channel and banks.

and (b) Manning ***n*** of 0.035 for both channel and banks [*Magirl et al*., 2008] (scenario 1). At the lower segment of the study reach, where our study site is located, the best fit for these discharges was scenario 2, especially for discharges $>3000\ m^3s^{-1}$; therefore, it was used later for all iterations of WSP's for all discharges up to 10,000 m^3s^{-1}. The downstream boundary conditions (DBC) were determined using the elevation of the measured high water marks of the May 2005 flood—1140 m^3s^{-1}. The resulting WSP of this flood calibrates the HEC-RAS WSP's (Figure 9). This WSP has a gradient of 0.0004, which was used as a DBC for the WSP's of all discharges including the 1884 high water marks (3540 m^3s^{-1}).

3.4. Flood Frequency Analysis Methods

We used the gaged annual peak discharge values from USGS gage no. 09180500 (Colorado River near Cisco, UT) to calculate the annual peak flows at the study site. The gaged record include 97 annual peak flows (1884, 1914–1917, 1923–2012) (Figure 4). The preliminary frequency analysis of the entire gaged record yielded similar magnitudes—2765 and 3500 m^3s^{-1} for return periods of 100 and 500 years, respectively. This result is probably related to the history of upstream regulation and water extraction. Therefore, only the 43 peaks from 1884 to 1960 were used for subsequent analysis because they represent the flow least affected by regulation, and thus more closely represents the natural flow on the Colorado River (Figure 4). The methodology of *Cudworth* [1989] was used to adjust the 43 peaks in the gaged record to the drainage area at the study site. The relationship assumes that the ratio of the peak discharges Q_1/Q_2 at the two locations is equal to the square root of their respective drainage areas $A_1^{0.5}/A_2^{0.5}$. The difference between the two drainage areas is 975 km^2—an increase of 1.6% only. The discharge values at the study site were used in the frequency analyses.

Because flow measurements in the gaged record at this station are generally labeled "good" or "fair," we assigned all values an uncertainty of 15%, the accepted uncertainty for good or fair measurements. The one exception is the exceptionally large peak flow in 1884, which is a historic peak (3540 m^3s^{-1}) that was not gaged. We assigned it an uncertainty of 25%, based on the measured gap between the actual elevation of the water surface as represented by the assumed driftwood of this flood and the dated SWD (Figure 10).

Our conservative flood frequency analysis uses only 18 paleofloods of the entire record and the estimated (unrecorded) 1921 flood. These floods were chosen because they could be distinguished from all other floods based on geochronology and the stratigraphic relationships. Flood deposits that could have been correlated to other deposits at different pits/sites, were not used in the flood-frequency analyses. Because slack-water deposits represent a minimum water surface elevation, paleofloods were assigned a discharge range with the minimum discharge value being the value obtained from hydraulic modeling. In keeping with a similar methodology as the gaged record, for floods over 3000 m^3s^{-1} the maximum value was 50% greater than the minimum, and the most likely value half way between the two values or 25% greater than the minimum, similar to the 1884 flood. For floods with discharge magnitudes less than 3000 m^3s^{-1}, the maximum discharge used was 30% greater than the minimum and the most likely values was 15% greater than the minimum, similar to

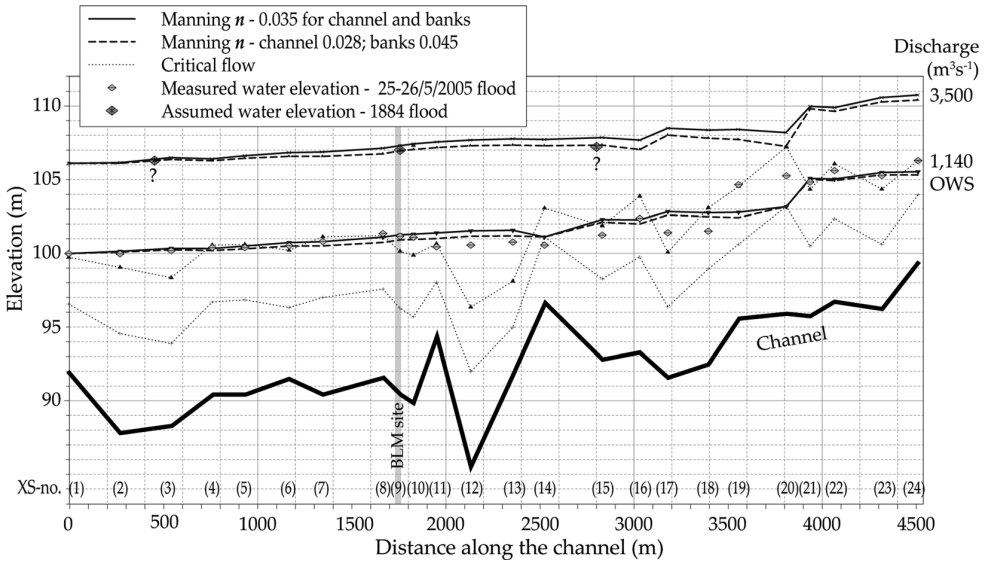

Figure 9. Water surface profiles (WSP) for peak discharges of 1140 and 3500 m^3s^{-1} along the study reach using HEC-RAS hydraulic program in relation to the measured water elevations of the 25–26 May 2005 flood—1140 m^3s^{-1} and for the assumed high water marks of the 1884 historical flood—3500 m^3s^{-1}. The iterations for each discharge include two roughness scenarios of Manning ***n*** coefficient: channel and banks—0.035 (scenario 1), and channel—0.028, banks—0.045 (scenario 2). The WSP of scenario 2 is the best fit for the measured points (shown in diamonds) along the lower segment cross sections (XS's) nos. 1–14. For XS's 1–10 only the best fit is scenario 1 (see Figure 8). For the high water marks of the 1884 flood—3500 m^3s^{-1}, the best fit is the WSP of scenario 2 due to the decrease of relative roughness with increasing water depth. The downstream boundary condition (DBC) for the 1140 m^3s^{-1} iteration is the elevation of the measured high water marks of the May 2005 flood at XS1. The measured elevations at the downstream cross sections form a WSP gradient of 0.0004. This gradient was used as a DBC for the WSP of the 1884 high water marks—3500 m^3s^{-1} for both scenarios. Note that XS-14 serves as control for the discharge of 1140 m^3s^{-1}, whereas XS-20 serves as control also for the discharge of 3500 m^3s^{-1}.

the documented 2005 flood. In the frequency model, all discharge values were assigned an equal weight. Similar methods and uncertainty determinations were used for an extensive paleoflood study in the Black Hills, South Dakota [*Harden et al.*, 2011]. Generally, the median of each geochronologically dated flood was the age used in the flood-frequency calculations. If two or more floods had the same age range, the ages used in the frequency analyses were evenly spaced in that range, since the number of floods per time period is more important in the frequency analysis than the exact ages of the floods.

Flood-frequency analyses for (a) the gaged record only, (b) the gaged plus paleoflood record for scenario 1, and (c) the gaged plus paleoflood record for scenario 2 were computed using the Bureau of Reclamation's FLQFRQ3 model [*O'Connell*, 1999; *O'Connell et al.*, 2002]. The FLDFRQ3 model uses a Bayesian approach [*O'Connell et al.*, 2002] with a maximum likelihood method [*Stedinger and Cohn*, 1986]. The FLDFRQ3 model allows for specification of uncertainties for magnitudes and timing of hydrologic events that arise due to flow-rate, stratigraphic, and chronologic uncertainties. The model also allows for nonexceedance bounds derived from paleoflood data. For this study, four bounds were used (Figure 10): two bounds are based on the documented elevations of (a) the largest paleoflood in the entire record and (b) the large 1884 flood which was used as a bound for the historical and systematic records. The other two bounds are based on the assumption that larger floods would have left stratigraphic evidence. These bounds are based on physical characteristics of the bank such as high bedrock ledge between pits 1 and 2 (bound c, Figure 10) and large boulders from the underlying gravel which separates between the two depressions and between pits 6 and 9 (bound d, Figure 10). Flood-frequency analyses were computed assuming log-Pearson Type III frequency distributions. The Weibull plotting position was used for graphical representations of results of flood-frequency analyses.

3.4.1. Limitations in the Frequency Analysis

The FLDFRQ3 model accounts for standard statistical uncertainties in sampling populations and for additional user-specified uncertainties in the timing and magnitude of individual paleofloods. The model also allows for user-specified characterization of the probability distribution function for flood-frequency analysis and for specifying uncertainty in the observational record. The model, however, cannot explicitly account

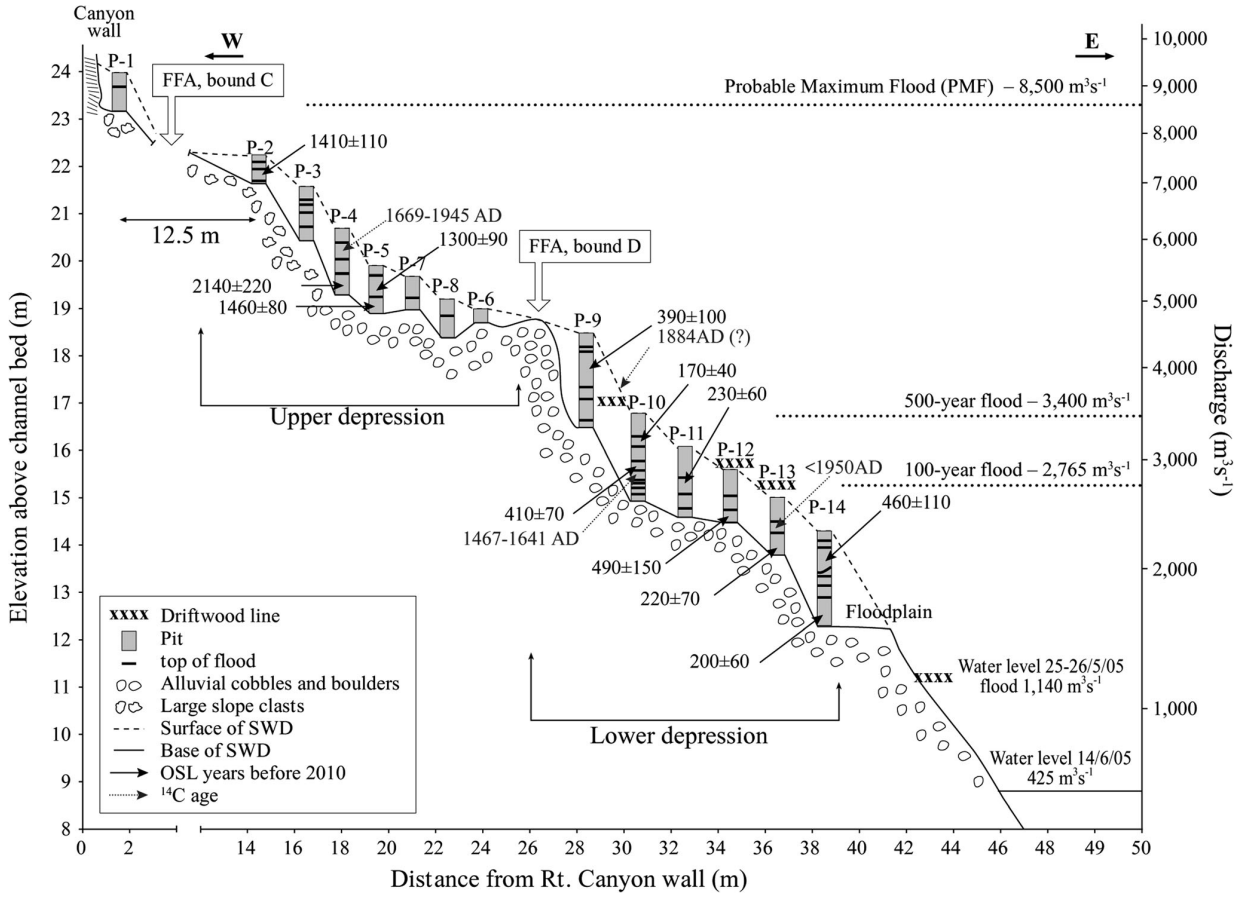

Figure 10. Cross section perpendicular to the Slackwater deposits (SWD) relict at the BLM-TO site including the elevation and horizontal locations of the pits and their associated peak discharges, ages of the paleoflood deposits, the OWS of 25–26 May 2005 flood (1140 $m^3 s^{-1}$), and the upper bounds for the flood frequency analysis. Note that: (a) the SWD trap is composed of two separate depressions—an upper depression (pits 2–8) and a lower depression (pits 9–14). (b) Pit no. 1 is separated and located at the base of a rocky bench of the canyon wall at an elevation of about 24 m above channel bed. (c) The ages of the flood deposits at the upper depression are older than at the lower depression representing older and larger floods. (d) The elevation and discharges for the various pits and flood deposits at the site including the 100 yr flood, the 500 yr flood and the PMF. (e) The OSL age of flood no. 5 in pit 14—460 ± 110 years came out older and does not follow the stratigraphy. This usually characterizes a nonhomogenous population which contains quartz grains that were not completely bleached.

for other factors or conditions that may affect both the analyses and the future recurrence of low-probability floods. Results of flood-frequency analyses may be affected by biases inherent in the stratigraphic approach as conducted for this study that possibly result in underestimating the number of recognized floods (i.e., not all flood units were used in the frequency analysis), and their associated magnitudes.

This frequency analysis does not address uncertainties related to nonstationary climatic trends or long-term changes in geomorphic and land-cover conditions. Thus, the flood-frequency estimates resulting from this study may not perfectly describe future flood recurrence. Although, in the United States, the log Pearson Type III (LP3) distribution is the federally suggested frequency distribution, this study did not assess the fit of the LP3 versus other frequency distributions for the Colorado River.

4. Results

4.1. Paleofloods and Slack-Water Deposits

The BLM-TO site is an overbank relict composed of two depressions within the underlying alluvial terrace, in which the SWD's were trapped and accumulated (Figure 10). The higher depression, represented by pits 2–8 is 18.9–22.2 m above channel bed, is relatively shallow (between 0.3 and 1.4 m deep). The lower

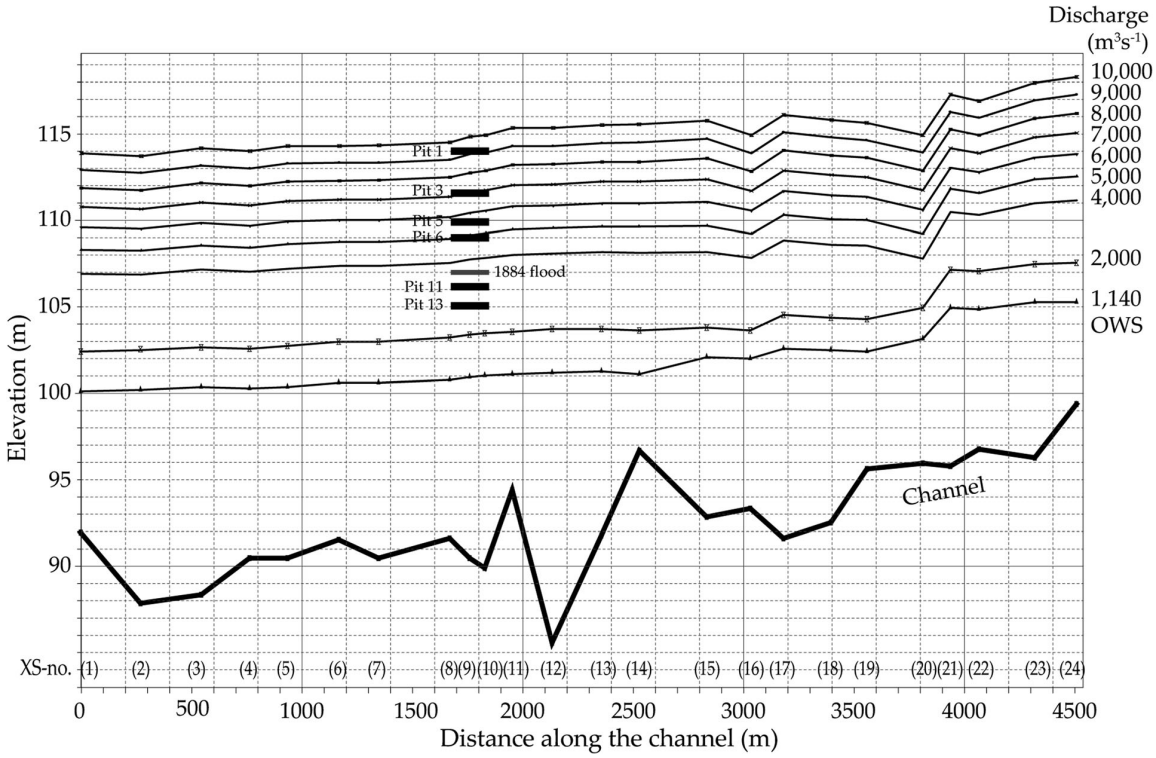

Figure 11. Water surface profiles (WSP) for peak discharges of 1140–10,000 m^3s^{-1} along the study reach using the HEC-RAS hydraulic program in relations to the top surface of pits 1,3,5,6,11,13 and the 1884 flood (3500 m^3s^{-1}). The downstream boundary conditions (DBC) are water surface gradient of 0.0004 based on the calibration shown in Figure 9 indicating that scenario 2—Manning ***n*** coefficients—channel—0.028, banks—0.045 is the best fit for the high discharges due to the decrease in relative roughness with increasing water depth. XS-20 serves as control discharges up to 6000 m^3s^{-1} and is subcritical close to critical for the larger discharges.

depression, represented by pits 9–14 located 12.9.−18.5 m above channel bed, is deeper (between 0.8 and 2.0 m). The uppermost SWD's were exposed in pit 1 located at the base of the rocky rim of the canyon (Figures 7 and 10) at an elevation of 23.4–24.0 m above channel bed.

The sedimentary units were separated into flood-related deposits. Criteria for separation between flood sedimentary units were: (a) abrupt changes in texture, structure, or color; (b) presence of organic layers, and (c) presence of gravelly slope deposits. Pits 1–8 (Figure 10) include 1–5 flood deposits, while pits 9–14 contain 3–9 flood deposits.

Correlation between flood layers in adjacent pits serve as a basis for the stratigraphy interpretation of the entire site, and is based on the properties of the sediments, the geometries of the various units, their lateral continuity, field relationships among the deposits, and numerical age dating.

The entire paleoflood record at the site consists of 44 paleofloods, 15 of which are evidenced by deposits at the upper depression, 27 at the lower depression, and two floods in the highest pit 1. A clear line of coarse driftwood consisting of large logs was documented at an elevation of about 17 m above channel bed. This driftwood line which occurs in other segments along the canyon was correlated to the 1884 flood (3540 m^3s^{-1}) based on historical descriptions of that flood and by relating its level to that indicated by the reconstructed peak discharge of 3500 m^3s^{-1} (Figure 9). A much lower driftwood line was emplaced by the observed and recorded flood of 25–26 May 2005 which had a peak discharge of 1140 m^3s^{-1} (Figures 9 and 11). This driftwood line was about 50 cm higher than the SWD that was emplaced by the same flood (Figures 7 and 10).

4.2. Dating

4.2.1. Radiocarbon

The results of the radiocarbon dating at the various pits are presented in Table 1. The radiocarbon age for unit 5 in pit 14—6275±160 years (Figure 10) indicates that it is much older than the entire paleoflood record, including the deposit that it overtops. This date probably results from the contribution of older organic material to the soil and therefore is considered as not reliable.

4.2.2. Luminescence Dating

Twelve samples from 11 pits were dated by the OSL method (Table 2). The ages for the SWDs range from several hundred years up to over 2000 years (Figure 10 and Table 2). The samples appear to cluster into two age groups, one older than 1300 years and the other younger than 490 years before 2010. The ages of the older samples, between 1300 and 2140 years, are well-constrained and have small uncertainties (sample errors of 5–10%). The samples $<$ 490 years show a large scatter of De values (samples errors of 17–32%), indicating that the sediments are not homogenous with respect to solar bleaching [*Clarke*, 1996]. Ages for these samples were calculated without obviously outlying old aliquots. Even so, the insufficient bleaching implies that the ages presented in Table 2 are maximum ages, and the timing of SWD deposition could be more recent.

4.3. Stratigraphy, Chronology, and Correlation of the Flood Deposits

The large number of dates provides a relatively high chronological resolution for this particular paleoflood record. The result is an improved stratigraphic interpretation and an unusually detailed history of the largest floods for the last two millennia.

The indicated record of paleoflood ages can be viewed as reliable because both the OSL and radiocarbon ages are generally in accordance with each other and with the paleoflood stratigraphy. Most of the older flood deposits $>$ 1000 years before 2010 occur within the upper depression (Figure 10), whereas the deposits in the lower depression are characterized by younger ages—$<$ 490 ± 150 yr. The uppermost flood deposit second flood from the top of pit 10 (Figure 10), was correlated to the historical 1884 AD (3540 m^3s^{-1}) based on the OSL age and the calculated peak discharge (3000–3180 m^3s^{-1}). This means that the difference between the coarse driftwood line and the SWD of the 1884 flood is between 1 and 1.5 m.

The two undated largest floods at the site—pit 1, floods 1 and 2 (Figure 10) with peak discharges of 9200 and 8910 m^3s^{-1} were correlated to the largest paleofloods (14,000 m^3s^{-1}) downstream at Lees Ferry dated to 350–750 AD [*O'Connor et al.*, 1994] (Figure 1). This correlation provides age estimates between 1660 and 1260 yr BP to the largest floods at our study site.

4.4. Hydraulic Analyses and Paleoflood Magnitudes

The reconstructed paleoflood record in the Upper Colorado River include 44 floods during the last 2140 ± 220 years. The elevation of the SWD'S is up to 24 m above channel bed (Figure 10). Comparative magnitude results of the various hydraulic analyses are presented in Table 3. All discharge calculations at the study site are calibrated by measured flows at the Dewey Bridge gauging station 30 km upstream (Figure 1).

Table 3. Summary of Paleofloods at the BLM-TO Site, Minimal Peak Stages, and Calculations of Minimal Peak Discharges Using Various Hydraulic Analyses

Location	Pits No.	No. of SWD Units	Stage Above Channel Bed (m)	Peak Discharge Slope-Area (m^3 s^{-1})	Peak Discharge HECRAS (m^3 s^{-1})	Peak Discharge HECRAS+ Underwater Data (m^3 s^{-1})
Base of rim	1	2	23.4–24.0	>10,000	8100–8300	[a]8500–8750 [b]8870–9200
Upper depression	2–8	15	18.9–22.2	5100–8700	4500–7400	[a]4530–7300 [b]4810–7660
Lower depression	9–14	27	12.9–18.5	2200–4600	1600–4200	[a]1650–4290 [b]1800–4550
Total	**1–14**	**44**	**12.9–24.0**	**2200–10,000**	**1600–8300**	[a]**1650–8750** [b]**1800–9200**

[a]Manning ***n*** – 0.035 channel and banks (Scenario 1).
[b]Manning ***n*** – 0.028 channel; 0.045 banks (Scenario 2).

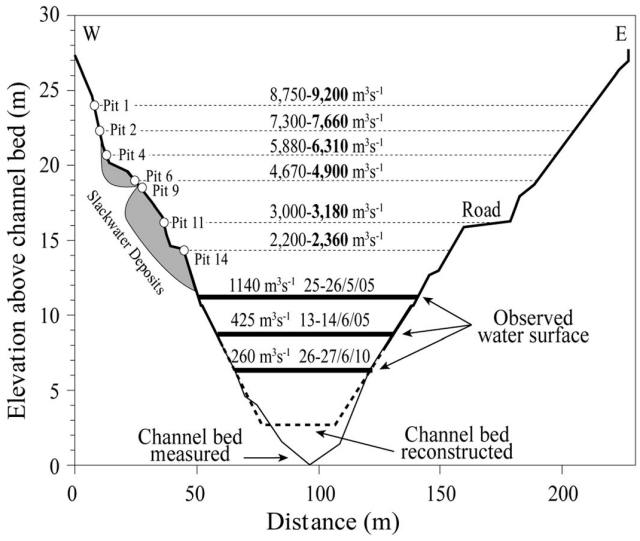

Figure 12. Cross section no. 9 across the Colorado River at the study site, elevations of the pits and the associated peak discharges using HECRAS hydraulic analysis and the observed water surfaces. The ranges of peak discharges are based on the two roughness scenarios of Manning ***n*** coefficient: channel and banks—0.035 (scenario 1), and channel—0.028, banks—0.045 (scenario 2), although the latter (in bold) is the best fit to the data. The location of the section is shown in Figures 6, 9, and 11. A detailed section across the site is shown in Figure 10.

The slope-area calculations of *Greenbaum et al*. [2006b] estimated the highest peak discharges as between $>2000\ m^3s^{-1}$ and up to $>10{,}000\ m^3s^{-1}$ (353,140 cfs). The step backwater HEC-RAS results reported here for the same data set are 15–20% lower and range from $>1600\ m^3s^{-1}$ up to $8300\ m^3s^{-1}$ (293,100 cfs). The HEC-RAS hydraulic analysis for the complete channel topography provides maximum peak discharge values of between 8910 and 9200 $m^3\ s^{-1}$ (314,650 and 324,900 cfs) (Figures 11–13) depending on the choice of Manning ***n*** values (Figures 8 and 12). The best fit to the data was produced by the lower Manning ***n*** coefficients (scenario 2), indicating that the discharge of $9200\ m^3s^{-1}$ is the most probable maximum peak discharge value for our study site.

The calculated peak paleovelocities for the two largest paleofloods in the record using slope-area method are 5.1–5.3 m s^{-1}. The HEC-RAS water surface profiles for these and other large discharges for the study reach indicate velocities in the subcritical flow regime. Supercritical conditions only occur at a few locations where the channel gradient abruptly increases due to cataracts, rapids, and narrow constrictions. These generally occur at the lower discharges (Figures 9 and 11), because at higher flows the cataracts can be deeply covered with water, thereby making the flow subcritical. All the iterations of water surface profiles indicate that cross section no. 20 serve as a control discharges up to 6000 m^3s^{-1}; larger discharges are

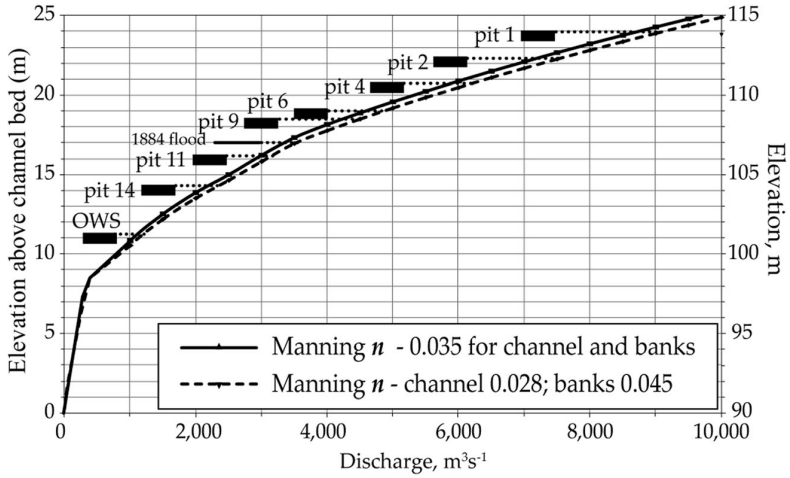

Figure 13. Rating curves for the paleoflood site (XS-9, Figures 11 and 12) for the two roughness scenarios of Manning ***n*** coefficient: channel and banks—0.035 (scenario 1), and channel—0.028, banks—0.045 (scenario 2) and the peak discharge determinations for the tops of pits 1, 2, 4, 6, 9, 11, 14, the historical 1884 flood and the observed 25–26 May 2005 flood (OWS).

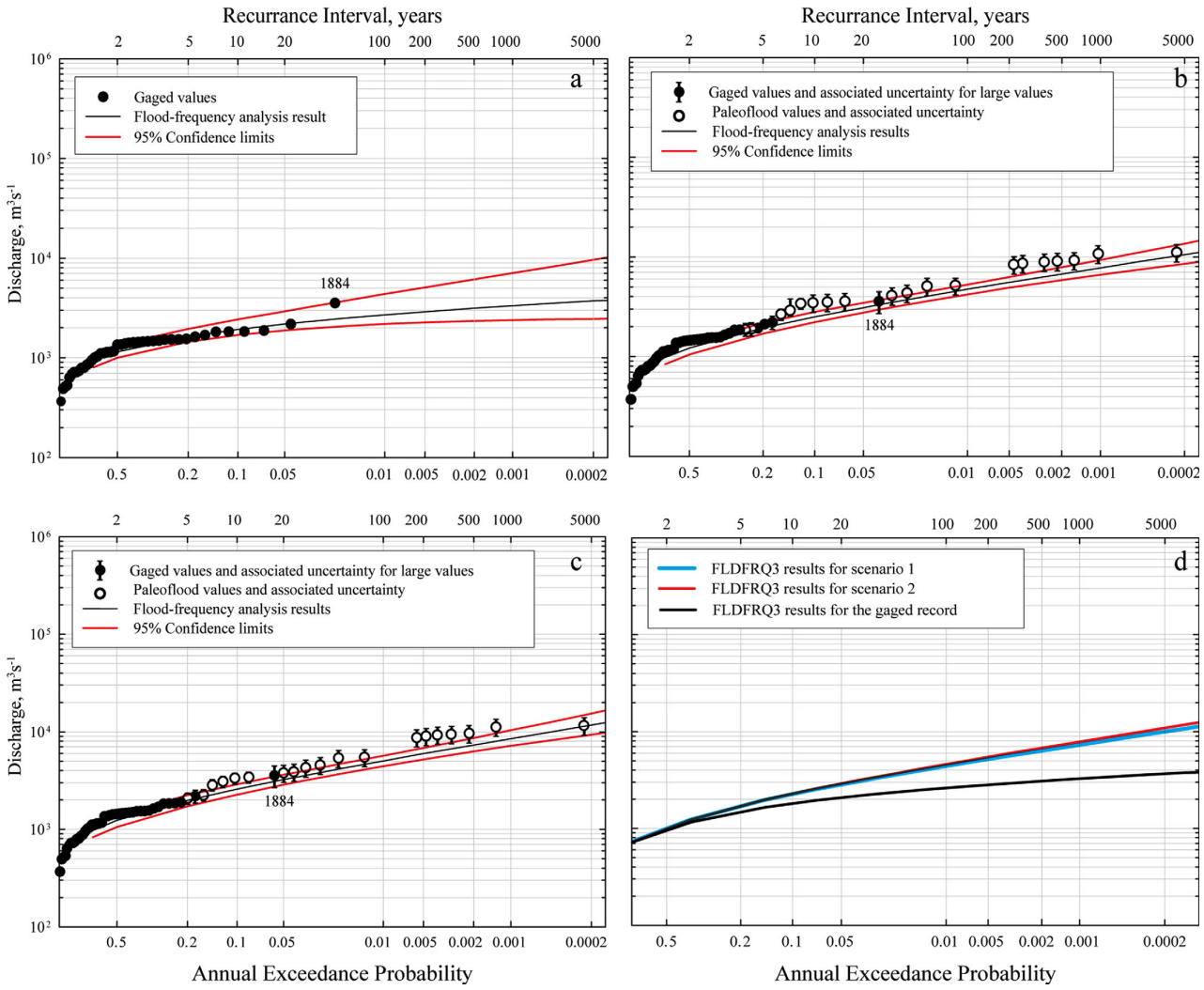

Figure 14. Results of flood frequency analyses at the Colorado River site using the FLDFRQ3 model for the (a) gaged record only (b) gaged and paleoflood data (scenario 1, 19 floods, 50% uncertainty) and (c) gaged and paleoflood data (scenario 2, 19 floods, 50% uncertainty) (d) Comparison between Figure 14(a) and Figure 14(c).

subcritical. Cross section no. 14 serves as a control for the lower discharges, but does not affect peak discharges > 2000 m^3s^{-1}, since it becomes covered with a thick layer of water (Figures 9 and 11).

Our 2010 survey shows that the underwater topography is continuous with the subaerial topography both in terms of the general morphology and the gradients of the banks. The maximum depth of the channel-bed below the water surface ranges between about 4 and 16 m (XS 12; Figure 9) for a discharge of 1140 m^3s^{-1}. At the paleoflood study site in XS-9 (Figures 9 and 12), the depth of the channel bed is about 11 m.

4.5. Flood Frequency Analysis

We found major differences between the results of the frequency analyses performed on the partial gaged record (1884–1960) (Figure 14a) versus the combination of the paleoflood and the gaged records – scenarios 1 and 2 (Figures 14b and 14c; Table 4). The 100 year flood based on the gaged record only is 2730 m^3s^{-1} versus 4670 and 4990 m^3s^{-1} for scenarios 1 and 2, respectively. The 500 year flood is 3185 m^3s^{-1} for the gaged record, 6675 m^3s^{-1} for scenario 1, and 7270 m^3s^{-1} for scenario 2. The 1000 year

Table 4. A Comparison Between Flood Frequency Results of the Present Study and the Previous Study by *Kenney* [2004] (Peak Discharge in m^3s^{-1})

Recurrence Interval (Years)	Gaged Record USGS) [*Kenney*, 2004]	Gaged Record (Present Study)	Paleoflood + Gaged Records (Present Study)	
			Scenario 1	Scenario 2
100	2765	2730	4670	4990
200		2930	5480	5910
500	3400	3185	6675	7270
1000		3365	7680	8440
5000		3750	10,425	11,675
PMF	8500			

flood is 3365 m^3s^{-1} for the gaged record, 7680 m^3s^{-1} for scenario 1 and 8440 m^3s^{-1} for scenario 2 (Figure 14d and Table 4).

5. Discussion

5.1. Hydraulics and Magnitudes

In natural channels for low discharges, the flows are usually close to critical, due to channel morphology—waterfalls, constrictions and control cross sections. For such flows, the significance of Manning ***n*** coefficient is minor because the water level is determined by the large number of the control sections. In the Upper Colorado River, this is probably the case for the lower discharges of up to 2000 m^3s^{-1} where the flows are close to critical. For the large discharges of the paleoflood record, which are characterized by a large rise in water stage and hydraulic radius, the flows are subcritical and Manning's ***n*** becomes somewhat more significant. *Enzel et al*. [1994] demonstrated that for large floods a change of $\pm$20% in ***n*** values produces a change of $< \pm$5% in the corresponding discharge. In the present study, a change in ***n*** values by $<$ 20% caused a difference of about 5–10% in the corresponding peak discharges (Figures 12 and 13; Table 3). A comparison of the iterations with different Manning ***n*** values for the largest flood shows that for the lower ***n*** coefficients (0.028 for the channel and 0.045 for the banks, scenario 2) the resulting peak discharge is 9200 $m^3\ s^{-1}$ in comparison to 8750 $m^3\ s^{-1}$ for the higher ***n*** coefficient (0.035 for channel and banks, scenario 1). Using the lower roughness coefficients, which we assume are more suitable for the channel characteristics of the lower segment (Figures 8, 9, and 11), especially for discharges $>$3000 $m^3\ s^{-1}$ for which roughness decreases with increasing water elevation, the minimum peak discharges are 9200 and 8910 m^3s^{-1} for the two largest floods during this period. These values exceed the USGS calculated Probable Maximum Flood (PMF) for the Moab Valley: 8500 m^3s^{-1} (300,000 cfs) [*Kenney*, 2004]. Another four floods exceeded a minimum peak discharge of 7000 m^3s^{-1} (about 247,200 cfs; Figure 10). The largest flood on the paleoflood record during the last 2140 $\pm$ 220 years with a peak discharges of 9200 $m^3\ s^{-1}$, is much larger than the largest 1884 AD historical flood (3500 $m^3\ s^{-1}$; Figure 11) by a factor of 2.6 and larger than the largest measured 1917 AD flood (2175 $m^3\ s^{-1}$) by a factor of 4.23. Nevertheless, this peak discharge does not exceed the envelope curve for the peak paleoflood discharges that have been documented for the Colorado River basin [*Enzel et al*., 1993].

5.2. Flood Frequency

Depending on the hydraulic scenario, about 34 floods during the last 2140 $\pm$ 220 years exceeded the 100 year flood estimated from the gaged record alone, 2765 m^3s^{-1} in *Kenney* [2004] and 2730 m^3s^{-1} for the present study (Table 4); for the same time period 26 floods exceeded the 500 year flood, 3400 m^3s^{-1} (Table 4) and two floods exceeded the PMF (8500 m^3s^{-1}) as calculated by the USGS for the Moab Valley [*Kenney*, 2004]. The similarity between the 100 and 500 year floods in the USGS estimates (Table 4) was explained mainly by the flow regulation during the past half a century, which reduced the peak magnitudes [*Kenney*, 2004]. This similarity was also evident in the present study even for lower probabilities.

The indicated anthropogenic effect on the frequency and magnitude of floods in the upper Colorado River implies that use of the systematic record alone severely underestimates the risk for floods with long-term recurrence intervals—$>$100 years (Figure 13). This probably occurs because: (1) There was an anthropogenic-related decrease in the measured peak discharges since the 1960's due to the decrease in

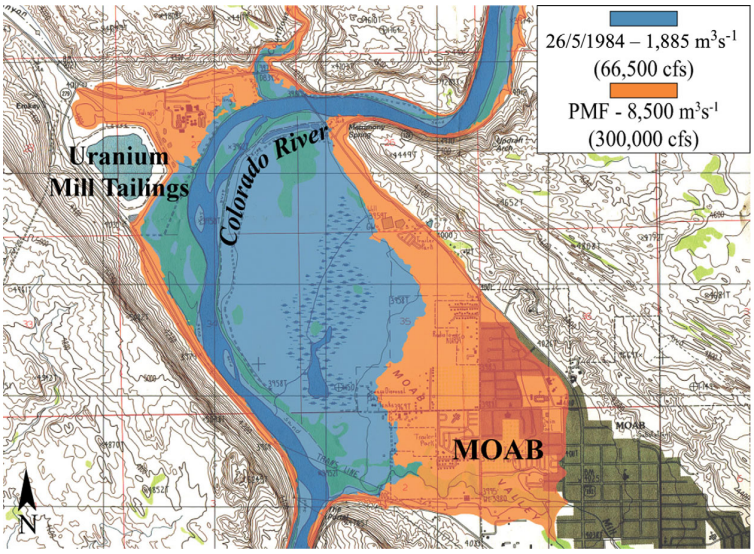

Figure 15. Inundation maps of the Moab Valley for the measured 26 May 1984 flood—1885 m^3s^{-1} (66,500 cfs) and for the estimated Probable Maximum Flood (PMF)—8500 m^3s^{-1} (300,000 cfs) [*Kenney*, 2004; *Weisheit and Fields*, 2006].

grazing, increase in agriculture, regulation of the river, and water extraction (Figure 5). The water extractions affect the discharge of the smaller and frequent flows and base-flows. For the Upper Colorado River—upstream of Cisco gage station, the annual water extractions equal to an annual flow of 71 m^3s^{-1} (J. Prairie, Bureau of Reclamation, personal communication, 2014). (2) The long-term paleoflood "window" records many more large floods with larger peak discharges, indicating that large, rare floods are more frequent than it appears in the systematic record, i.e., that the large floods are not represented "properly" in the systematic record. (3) A possible but limited climatic change during the last 100 years might be represented in the systematic record as a part of the decrease of the maximum annual peak discharge (Figure 4), although it is not recorded in the rainfall record of Moab (Figure 3).

Inundation maps of the Moab Valley for the measured 26 May 1984 flood—1885 m^3s^{-1} (66,500 cfs) and estimated for the Probable Maximum Flood (PMF)—8500 m^3s^{-1} (300,000 cfs) [*Kenney*, 2004; *Weisheit and Fields*, 2006] are presented in Figure 15. These show that floods with the PMF discharge, which based on the present study has a frequency of about 1000 years, and even much smaller floods, can inundate the town of Moab and much of the Moab Valley, also posing severe risk to the uranium mill tailings stored just north of the town.

5.3. Probable Maximum Flood Considerations

The Probable Maximum Flood is generally defined as, ". . .the flood that may be expected from the most severe combination of critical meteorological and hydrologic conditions that are reasonably possible in a given drainage area" [*Brekke et al*., 2009, p. 20]. This concept is invoked in engineering practice for high hazard dams to provide, ". . .the design standard as a risk-adverse approach to minimizing the potential loss to human life" [*Raff*, 2013, p. 37]. In regard to paleoflood hydrology, the U.S. Army Corps of Engineers (USACE) holds, ". . .if the decision leads to design or modification of a high hazard dam, then the utility of paleoflood information is minimal, as the current design standard is based on the Probable Maximum Floods (PMFs)" [*Raff*, 2013, p. ix]. This conclusion contrasts with engineering practice in the U.S Bureau of Reclamation (USBR), which, in much the same way that it uses paleoseimological information to evaluate extreme earthquake risk to high hazard dams, makes extensive use of paleoflood hydrological information in evaluating potential extreme flooding risk to such dams [*Levish*, 2002; *U.S. Bureau of Reclamation Reclamation*, 2003]. Similarly, the U.S. Geological Survey (USGS) adopted paleoflood hydrology for flood frequency analysis and incorporated it into their methodologies [e.g., *Jarrett*, 1991; *Harden et al*., 2011].

The differences between USBR and USACE engineering practice reflect basic philosophical differences, respectively, between a risk-based viewpoint (USBR and USGS) that attempts to evaluate probabilities for

even the most extreme flood magnitudes and a deterministic viewpoint (USACE) that claims to achieve the maximum practical safety by applying knowledge of what theory can provide as the most severe flood-generating conditions that could occur at a particular site. A possible role for paleoflood hydrology was proposed by the *U.S. National Research Council* [1985, p. 235], as follows: "When such techniques (i.e., paleoflood hydrology) are applicable, they should be used to demonstrate that calculated PMFs are credible and are neither unreasonably large nor small." The results of the present study, which finds paleoflood exceedances of the PMF for the Upper Colorado River, might be considered in the light of this recommendation and the questions that are raised in regard the goal of minimizing potential loss to human life. What should be done if a stipulated PMF value (what is theorized to be the flood that will result from the "most severe combination of critical meteorological and hydrologic conditions that are reasonably possible") is discovered to be contrary to what actually exists in nature?

5.4. Future Flood Scenarios and Nonstationarity Considerations

A current concern in regard to extreme flooding is that of posing future flood scenarios, given that there will be major future changes in climate and land use. One might ask, as did one reviewer of this paper, why a long-term paleoflood record might be used in regard to flood mitigation when it is known that climate and land use were different in the past. Therefore, a very long record of extreme flooding, such as the one documented by the present study, might improve the statistical analysis, but the actual floods in this record were likely subject to potentially very different climatic and environmental conditions than those of today.

Making this point another way, one might argue, as did this one reviewer, that best engineering practice might hold that, despite the limited time sampling of floods, one should base hazard mitigations on the relatively short flood records of gaging stations, since the floods that they document will have occurred during the climatic and environmental conditions of the present. However, this argument assumes that the climatic and environmental conditions characterizing today's short-term gage records, will remain the same into the future. Thus, the question of climate and land-use change applies to all risk analyses based on all real-world flooding data, not merely to paleoflood data. Moreover, in the highly variable, flood regimes of the arid and semiarid southwestern U.S., it is highly likely that the short systematic gaging records will not sample the occurrence of very large, rare floods. Because the systematic gage record is necessarily a "short time window," longer records are needed to put this record in proportion to the longer timescale. As illustrated by the present study, paleoflood hydrology can provide the means of sampling the largest floods to have occurred in a basin and also documenting the minimum number of very large floods that have occurred during a certain period.

These are interesting and important questions, but they are engineering questions addressed at achieving mitigation or design criteria in regard to future flooding. The present paper is not directed at making prognostications about the future; it does not seek to provide criteria for engineering designs. Paleoflood hydrology, like human history, does not generate "scenarios" for future flooding; the latter are commonly produced as the deductive output ("predictions" in a logical sense) from mathematical modeling combined with necessary assumptions. Like human history, paleoflood hydrology provides information on events that have actually occurred, and thereby can demonstrate what actually can occur. The goal is scientific, in this case to document and understand a record of the extreme flooding that nature has generated for the Upper Colorado River over a 2000 year time scale. This natural record was subjected to flood-frequency analysis by the same kind of procedures that are used to analyze the much shorter records that are typical of stream gages. Moreover, the similarity of statistical analysis promotes objective comparisons to be made between the 2000 year nature flood record and a century-scale gage record. How such results might be interpreted in regard to future flooding is a matter of engineering judgment that is beyond the scope of the present paper.

Engineers interested in the general issue of dealing with hydroclimatically induced nonstationarity in flood-frequency analysis can find discussions in *Redmond et al*. [2002] and *Frances* [2004]. The issue is placed in the context of quantitative paleoflood hydrology by *Benito and O'Connor* [2013].

There certainly is a pressing scientific issue in trying to understand the ways in which climate and land use affect extreme flooding. Moreover, real-world evidence of that flooding (not just model simulations) is absolutely essential, especially for the long timescales that actually will include some of the types of extreme flood events that might possibly occur in the future [*Merz et al*., 2014]. The extreme events of the past are

indeed important indicators of what the atmosphere-catchment system is capable of. They have left evidence in the landscape of the occurrence of a real event. Floods—by their very nature—are rare events, hence there is a need to identify them in all temporal contexts (paleo, historical, and systematically gauged) and explain them from a mechanistic understanding of causal drivers [*Merz et al*., 2014].

Nonstationarity for flood characteristics involves violations of the usual assumption that flood-generating processes will remain constant in time, and that flood probabilities will correctly portray their long-term natural variability [*Merz et al*., 2014]. To assume that changes in climate or land-use will invalidate the role of long-term records for future, hazard designation presumes that there is little or no information on those changes. It is the goal of science to discover what those changes actual are, and to use resulting information to improve understanding, i.e., to discover and understand how and why these changes arise. Paleoflood records, combined with other information on paleoclimates, provide what *Merz et al*. [2014, p. 1573) term, ". . .evidence in the landscape of. . .real event[s]." There is a large scientific literature on the relationships between flooding and climate in the southwestern U.S., and building upon this base would be important to follow-on research related to the discoveries reported in this paper.

For example, *Ely et al*. [1993], in an extensive paleofloods study of >250 paleofloods from the southwestern U.S., found that the occurrence of extreme floods during the last 500 years was 190 of the 250 floods (about 76%). Similarly, at our site, about 32 floods of the 44 reconstructed paleofloods (73%) occurred during the last 500 years. The 5000 year record of *Ely et al*. [1993] uses time increments of 200 years and show that peaks in frequency and magnitudes of paleofloods are concentrated at around 1000 years BP and during the last 500 years, especially at the late 1800s and early 1900s. Their occurrence was correlated to transitions between cool and warmer climatic conditions, i.e., between a brief cold period around 1000 years BP and the following Medieval Warm Period (1100–1300 A.D.) and between the cold Little Ice Age (LIA; 1500–1800 A.D.) and the following, much warmer, 19th and 20th centuries. These floods are highly correlated to increased recurrence and intensity of El Nino events [*Ely et al*., 1993; *Hereford*, 2002]. The LIA was also a period of relatively high frequency of extreme floods but with lower peaks [*Ely et al*., 1993]. At our site, most of the floods occurred during the last 500 years, and only about a quarter earlier—between about 2140 and 500 years.

6. Summary

1. Our paleoflood hydrology study at the present site documented 44 floods during the last 2140 ± 220 years with peak discharges ranging from 1800 m^3s^{-1} up to 9200 m^3s^{-1} (about 324,900 cfs). Most of these floods occurred during the last 500 years.

2. The age dating for our study was done mainly by OSL, which provides consistent ages for the floods at the site. In general, the ages are in agreement with the stratigraphy of the site and with radiocarbon dates from the same units. Therefore, this method offers an efficient tool of dating almost every flood deposit along the Colorado.

3. Our results indicate that very large floods (a) are much more frequent than indicated by previous estimations which were based exclusively on analysis of the measured, systematic gage record, and (b) their frequency has increased during the last 500 years. This is in agreement with other studies in the southwestern U.S. that indicate an increase of extreme floods occurrence. The average long-term occurrence of large, rare floods is not adequately represented in the gaged record. At least, two large floods (9200 and 8910 m^3s^{-1}) occurred during two millennium recording period, and both these floods had discharges that exceeded the probable maximum flood (PMF; 8500 m^3s^{-1}—300,000 cfs). Another four floods exceeded 7000 m^3s^{-1} (about 247,200 cfs).

4. According to our paleoflood hydrology frequency analysis, the discharge of the previously presumed PMF, 8500 m^3s^{-1}, actually has a recurrence interval of about 1000 years, whereas the largest historical 1884 flood, 3540 m^3s^{-1}, has a recurrence interval of <100 years.

5. The gaged record (1914–2012) is biased toward low flows. This trend is clear for the period after 1960, and it can be attributed to a change in land-use from grazing to agriculture in the upper Colorado basin. Related to this is the regulation of the river flows and the extraction of large water amounts for cultivation. Even when eliminating the post-1960 period, the gaged record from 1914 to 1960, when used as the sole

basis for a flood frequency analysis, provides only the very low values of 2730 $m^3s^{-1}$and 3185 m^3s^{-1} for the 100 yr and 500 yr floods, respectively.

6. Our conservative results indicate that the previous flood frequency analysis for the Moab Valley based on the gaged record alone greatly underestimates the frequencies of extreme floods on a river that is critical to the water security of the nation. The paleoflood hydrology frequency analysis indicates the following flood risk values for the Moab valley: 100 yr flood 4670–4990 m^3s^{-1}; 500 yr flood 6675–7270 m^3s^{-1}; 1000 yr flood 7680–8440 m^3s^{-1}.

Acknowledgments
This first stage of this study was funded by the MTA Fund to Living Rivers in the framework of the "Moab Mill Project: A technical report toward reclaiming Uranium Mill Tailings along the Colorado River in Grand County, Utah". The second stage was funded by the U.S. Bureau of Reclamation with the project: "Impact of Climate Change on Extreme Floods in the Western U.S.," Agreement No. 09-FC-81-1503), to Victor R. Baker, The University of Arizona. We thank Wildland Scapes for helping in digging the pits and Tag-A-Long Expeditions for helping with the boats. The figures were drawn by Noga Yoselevich, the Cartography Laboratory of the Dept. of Geography and Environmental Studies, University of Haifa, Israel.

References

Aitken, M. J. (1998), *An Introduction to Optical Dating*, Oxford Univ. Press, Oxford.
Anderson, R. Y. (1993), Long-term changes in the frequency of occurrence of El Nino events, in *El Nino: Historical and Paleoclimatic Aspects of the Southern Oscillation*, edited by H. Diaz and V. Markgraf, pp. 193–200, Cambridge Univ. Press, Cambridge, U. K.
Baker, V. R. (1975), Flood hazards along the Balcones Escarpment in central Texas: Alternative approaches to their recognition, mapping and management, *Bur. of Econ. Geol. Circ. No. 75–5*, 22 pp., Univ. of Tex., Austin, Tex.
Baker, V. R. (1987), Paleoflood hydrology and extraordinary flood events. *J. Hydrol.*, *96*, 79–99.
Baker, V. R. (2003), A bright future for old flows: origins, status and future of paleoflood hydrology, in *Paleofloods, Historical Data and Climatic Variabillity: Applications in Flood Risk Assessment*, edited by V. R. G. Thorndycraft et al., CSIC Publication, Madrid, Spain, pp. 13–18.
Baker, V. R. (2006), Palaeoflood hydrology in a global context, *Catena*, *66*, 141–145.
Baker, V. R. (2008), Paleoflood hydrology: Origin, progress, prospects, *Geomorphology*, *101*, 1–13.
Baker, V. R. (2013), Global late quaternary fluvial paleohydrology with special emphasis on paleofloods and megafloods, in *Treatise on Geomorphology*, edited by J. Shroder, vol. 9, *Fluvial Geomorphology*, edited by E. E. Wohl, pp. 511–527, Academic, San Diego, Calif.
Baker, V. R., and R. C. Kochel (1988), Flood sedimentation in bedrock fluvial systems, in *Flood Geomorphology*, edited by V. R. Baker, R. C. Kochel, and P. C. Patton, pp. 123–128, John Wiley, N. Y.
Baker, V. R., Kochel, R. C., and P. C. Patton (1979), Long-term flood-frequency analysis using geological data, *IAHS AISH Publ.*, *128*, 3–9.
Baker, V. R., G. Pickup, and H. Polach (1985), Radiocarbon dating of flood events, Katherine Gorge, Northern Territory, Australia, *Geology*, *13*, 344–347.
Benito, G., and J. E. O'Connor (2013), Quantitative paleoflood hydrology, in *Treatise on Geomorphology*, edited by J. Shroder, vol. 9, *Fluvial Geomorphology*, edited by E. E. Wohl, pp. 459–474, Academic, San Diego, Calif.
Benito, G., Y. Sanchez-Moya, and A. Sopena (2003), Sedimentology of high-stage flood deposits of the Tagus River, central Spain, *Sediment. Geol.*, *157*, 107–132.
Benito, G., et al (2004), Use of systematic, palaeoflood and historical data for the improvement of flood risk estimation. Review of scientific methods, *Nat. Hazards*, *31*, 623–643.
Brekke, L. D., J. E. Kiang, J. R. Olsen, R. S. Pulwarty, D. A. Raff, D. P. Turnipseed, R. S. Webb, and K. D. White (2009), Climate change and water resources management: A federal perspective, *U.S. Geol. Surv. Circ.*, *1331*, 53 p.
Bronk Ramsey, C. (2009), Bayesian analysis of radiocarbon dates, *Radiocarbon*, *51*(3), 1023–1045.
Bronk Ramsey, C. (2013), *OxCal 4.2, Web Interface Build No. 78*, Oxford University, U. K.
Cayan, D. R., and R. H. Webb (1993), El Nino/Southern Oscillation and streamflow in the western United States, in *El Nino: Historical and Paleoclimatic Aspects of the Southern Oscillation*, edited by H. Diaz and V. Markgraf, pp. 29–68, Cambridge Univ. Press, Cambridge, U. K.
Clarke, M. (1996), IRSL dating of sands: bleaching characteristics at deposition using single aliquots, *Radiat. Meas.*, *26*, 611–620.
Cudworth, A. G. (1989), *Flood Hydrology Manual*, 243 p., U.S. Dep. of Interior, Bur. of Reclam., Denver, Colo.
Dickinson, W. E. (1944), Summary of records of surface waters at base stations in Colorado River Basin 1891–1938, *U.S. Geol. Surv. Water Supply Pap., 918*, 274 p.
Ely, L. L., and V. R. Baker (1985), Reconstructing paleoflood hydrology with slackwater deposits, Verde River, Arizona, *Phys. Geogr.*, *6*, 103–126.
Ely, L. L., R. H. Webb, and Y. Enzel (1992), Accuracy of post-bomb ^{137}Cs and ^{14}C in dating fluvial deposits. *Quat. Res.*, *29*, 2287–2297.
Ely, L. L., Y. Enzel, V. R. Baker, and D. R. Cayan (1993), A 5000-year record of extreme floods and climate change in the Southwestern United States. *Science*, *262*, 410–412.
Ely, L. L., Y. Enzel, and D. R. Cayan (1994), Anomalous North Pacific circulation and large winter floods in the southwestern United States, *J. Clim.*, *7*, 977–987.
Enzel, Y., L. L. Ely, P. Kyle House, and V. R. Baker (1993), Paleoflood evidence for a natural upper bound to flood magnitudes in the Colorado River Basin, *Water Resour. Res.*, *29*(7), 2287–2297.
Enzel, Y., L. L. Ely, J. Martinez-Goytre, and R. Gwinn Vivian (1994), Paleofloods and a dam-failure flood on the Virgin River, Utah and Arizona, *J. Hydrol.*, *153*, 291–315.
Frances, F. (2004), Flood frequency analysis using systematic and non-systematic information, in *Systematic, Palaeoflood and Historical Data for Improvement of Flood Risk Estimation*, edited by G. Benito and V. R. Thorndycraft, pp. 55–70, CSIC, funded by the European Commission SPHERE, Madrid, Spain.
Fuller, J. E. (1987), Paleoflood hydrology of the alluvial Salt River, Tempe Arizona, MSc. thesis, 69 pp., Dept. of Geosci., Univ. of Ariz., Tucson, Ariz.
Greenbaum, N., A. P. Schick, and V. R. Baker (2000), The paleoflood record of a hyperarid catchment, Nahal Zin, Negev Desert, Israel, *Earth Surf. Processes Landforms*, *25*, 951–971.
Greenbaum, N., A. Ben-Zvi, I. Haviv, and Y. Enzel (2006a), The hydrology and paleohydrology of the Dead Sea tributaries, in *New Frontiers in Dead Sea Paleoenvironmental Research*, edited by Y. Enzel, A. Agnon, and M. Stein, *Geol. Soc. Am. Bull.*, 401, 63–94.
Greenbaum, N., J. Weisheit, T. Harden, and J.C. Dohrenwend (2006b), Paleofloods in the Upper Colorado River near Moab, Utah, in *The Moab Mill Project, A Technical Report Toward Reclaiming Uranium Mill Tailings along the Colorado River in Grand County, Utah*, pp. 13–30, edited by J. Weisheit, and S. M. Fields, Living Rivers, Moab, Utah.
Harden, T. M., J. E. O'Connor, D. G. Driscoll, and J. F. Stamm (2011), Flood-frequency analyses from paleoflood investigations for Spring, Rapid, Boxelder, and Elk Creeks, Black Hills, Western South Dakota, *U.S. Geol. Surv. Sci. Invest. Rep., 2011–5131*, 136 pp.

Hereford, R. (2002), Valley-fill alluviation during the Little Ice Age (ca. A.D. 1400–1880), Paria River basin and southern Colorado Plateau, United States. *Geol. Soc. Am. Bull.*, *114*(12), 1550–1563.
House, P. K, R. H., Webb, V. R. Baker, and D. R. Levish, (Eds.) (2002), *Ancient Floods, Modern Hazards: Principles and Applications Of Paleoflood Hydrology, Water Sci. Appl. Ser.*, vol. 5, 385 pp., AGU, Washington D. C.
Hydrologic Engineering Center (2005), *HEC-RAS: Water River Analysis System, Version 3.1.3*, U.S. Army Corp. of Eng., Davis, Calif.
Jarrett, R. D. (1991), Paleohydrology and its value in estimating floods and droughts, in *National Water Summary 1988-89—Hydrologic Events and Floods and Droughts*, compiled by R. W. Paulson et al., *U.S. Geol. Surv. Water Supply Pap., 2375*, 105–116.
Kenney, T. A. (2004), Initial-phase investigation of multi-dimensional streamflow simulations in the Colorado River, Moab Valley, Grand County, Utah. *U.S. Geol. Surv. Sci. Invest. Rep., 2005–5022*, 69 p.
Kochel, R. C., and V. R. Baker (1982), Paleoflood hydrology, *Science*, *215*, 353–361.
Kochel, R.C., and V.R. Baker, (1988), Paleoflood analysis using slackwater deposits, in *Flood Geomorphology*, edited by V. R. Baker, R. C., Kochel, and P. C. Patton, pp. 357–376, John Wiley, N. Y.
Kochel, R. C., V. R. Baker, and P. C. Patton (1982), Paleohydrology of southwestern Texas, *Water Resour. Res.*, *18*(4), 1165–1183.
Levish, D. R. (2002), Paleohydrologic bounds: Non-exceedance information for flood hazard assessment, in *Ancient Floods, Modern Hazards: Principles and Applications of Paleoflood Hydrology, Water Sci. Appl. Ser.,* vol. 5, pp. 175–190, edited by P. K. House et al., AGU, Washington, D. C.
Magirl, C. S., M. J. Breedlove, R. H. Webb, and P. G. Griffiths (2008), Modelling water-surface elevations and virtual shorelines for the Colorado River in Grand Canyon, Arizona, *U.S. Geol. Surv. Sci. Invest. Rep., 2008–5075*, 32 pp.
Merz, B., et al. (2014), Floods and climate: Emerging perspectives for flood risk assessment and management, *Nat. Hazards Earth Syst. Sci.*, *2*, 1559–1614.
Murray, A., and A. G. Wintle (2000), Luminescence dating of quartz using an improved single-aliquot regenerative-dose protocol, *Radiat. Meas.*, *32*, 57–73.
O'Connel, D. R. H. (1999), *FLDFRQ3 User's Guide, Release 1.1*, 19 p., U.S. Bur. of Reclam.
O'Connel, D. R. H., D. A. Ostenna, D. R. Levish, and R. E. Klinger (2002), Bayesian flood frequency analysis with paleohydrologic bound data, *Water Resour. Res.*, *35(5)*. doi:10.1029/2000WR000028.
O'Connor, J. E., and R. H. Webb (1988), Hydraulic modelling for paleoflood analysis, in *Flood Geomorphology*, edited by V. R. Baker, R. C. Kochel, and P. C. Patton, pp. 383–402, John Wiley, N. Y.
O'Connor, J. E., R. H. Webb, and V. R. Baker (1986), Paleohydrology of pool-and-riffle pattern development: Boulder Creek, Utah, *Geol. Soc. Am. Bull.*, *97*, 410–420.
O'Connor, J. E., L. L. Ely, E. Wohl, L. E. Stevens, T. S. Melis, V. S. Kale, and V. R. Baker (1994), A 4500-year record of large floods on the Colorado River in the Grand Canyon, *Arizona. J. Geol.*, *102*, 1–9.
Partridge, J. B., and V. R. Baker (1987), Paleoflood hydrology of the Salt River, central Arizona, *Earth Surf. Processes Landforms*, *12*, 109–125.
Patton, P. C., V. R. Baker, and R. C. Kochel (1979), Slack-water deposits: A geomorphic technique for the interpretation of fluvial paleohydrology, in *Adjustment of the Fluvial System*, edited by D. D. Rhodes and G. P. Williams, pp. 225–253, Kendall/Hunt, Dubuque, Iowa.
Porat, N. (2002), Analytical procedures in the Luminescence dating laboratory Geological Survey of Israel, *Tech, Rep. TR-GSI/2/2002* [in Hebrew], Israel Geological Survey, Jerusalem, Israel, 44 pp.
Raff, D. (2013), Appropriate application of paleoflood information for the hydrology and hydraulics decisions of the U.S. Army Corps of Engineers, *Report CWTS 2013-2*, 45 p., U.S. Army Corp. of Eng.
Redmond, K. T., Y. Enzel, P. K. House, F. Bondi, (2002), Climate variability and Frequency at decadal to millennial time scales, in *Ancient Floods, Modern Hazards: Principles and Applications of Paleoflood Hydrology, Water Sci. Appl. Ser., 5*, pp. 21–45, edited by P. K. House et al., AGU, Washington, D. C.
Stedinger, J. R., and T. A. Cohn (1986), Flood frequency analysis with historical and paleoflood information, *Water Resour. Res.*, *22*(5), 785–793.
Thorndycraft, V. R., G. Benito, M. C. Llasat, and M. Barriendos, (2003), *Paleofloods, historical data and climatic variabillity: applications in flood risk assessment*, Proceedings of the PHEFRA international workshop, Barcelona 2002, 378 p., CSIC Publication, Madrid, Spain.
U. S. Bureau of Reclamation (2003), *Flood Hazard Analysis: Seminoe and Glendo Dams Kendrick Project and Pick Sloan Missouri Basin Program, Wyoming*, Tech. Serv. Cent., Denver.
U. S. National Research Council (1985), *Safety of Dams: Flood and Earthquake Criteria*, 176 p., Natl. Acad. Press, Washington, D. C.
Webb, R. H., J. E. O'Connor, and V. R. Baker (1988), Paleohydrologic reconstruction of flood frequency on the Escalante River, south central Utah, in *Flood Geomorphology*, edited by V. R. Baker, R. C. Kochel, and P. C. Patton, pp. 403–418, John Wiley, N. Y.
Webb, R. H., and J. L. Betancourt (1992), Climatic variability and flood frequency of the Santa Cruz River, Pima County, Arizona. *U.S. Geol. Surv. Water Supply Pap.*, 2379, 40 p.
Webb, R. H., and R. D. Jarrett (2002), One-dimensional estimation techniques for discharges of paleofloods and historical floods, in *Ancient Floods, Modern Hazards: Principles and Applications of Paleoflood Hydrology, Water Sci. Appl. Ser.*, vol. 5, pp. 111–126, edited by P. K. House et al., AGU, Washington, D. C.
Webb, R. H., D. E. Boyer, L. Orchard, and V. R. Baker (2001), Changes in riparian vegetation in the southwestern United States: Floods and riparian vegetation on the San Juan River, southeastern Utah, *U.S. Geol. Surv. Open File Rep., OF 01–314*, 25 pp.
Webb, R. H., J. Belnap, and J. Weisheit (2004), *Cataract Canyon*, 268 p., Univ. of Utah Press, Salt Lake City, Utah.
Weisheit, J. S. and S. M. Fields (2006), *The Moab Mill Project, A technical report towards reclaiming uranium mill tailings along the Colorado River in Grand County, Utah*, 30 pp., Living Rivers, Moab, Utah.
Wohl, E. E. (1998), Uncertainty in flood estimates associated with roughness coefficient. *J. Hydraul. Eng.*, *124*, 291–223.
Woolley, R. R. (1946), Cloudburst floods in Utah—1850–1938. *U.S. Geol. Surv., Water Supply Pap., 994*, 127 pp.